https://doi.org/10.5194/egusphere-2026-3763
Preprint. Discussion started: 21 July 2026

The use of remote sensing for studying environmental changes in a palsa mire zone of Northern Finland in the period 1985–2024

Małgorzata Szczepańska[1], Sebastian Czapiewski[1], Magdalena Suchora[2], Danuta Szumińska[1]

[1] Faculty of Geographical Sciences, Kazimierz Wielki University, 8 Kościeleckich Sq., 85-033 Bydgoszcz, Poland
[2] Institute of Earth and Environmental Sciences, Maria Curie-Skłodowska University, al. Kraśnicka 2d, 20-718 Lublin, Poland

Correspondence to: Małgorzata Szczepańska (m.szcz@ukw.edu.pl) and Danuta Szumińska (dszum@ukw.edu.pl)

Abstract

The palsa mires – hummocks with a permafrost core – of northern Finland are among the southernmost periglacial features in the Northern Hemisphere and mark the southern boundary of permafrost range. The rapid warming of circumpolar regions demands a better understand of the complex of environmental changes in the marginal permafrost zone. The study aims to investigate changes in selected environmental features (vegetation, water conditions and land moisture) in northern Finland in the years 1985–2024 using Landsat satellite data, with particular emphasis on the differences taking place in palsa mires. The calculated spectral indices NDVI, NDWI, MNDWI, NDMI and LST were analysed in relation to each other and to environmental data. The analysis of changes in spectral indices over time showed a small but systematic increase in the vegetation index value, an increase in soil moisture, and varied responses in indices related to surface water. Principal component analysis (PCA), linear mixed-effects models (LMM) and redundancy analysis (RDA) indicated the multidimensional structure of remote sensing indices and revealed the main environmental factors determining changes in vegetation and moisture in the study area. One of the main predictors differentiating the spectral response was determined to be palsa mires, which differed from mineral soils, but also from other organic soils. The results confirmed the effectiveness of RS and multispectral indices based on Landsat data for studying environmental changes, while indicating the need for multidimensional analyses that include various indicators and local environmental predictors.

1 Introduction

One of the most characteristic features of the northern European environment is its extensive peatlands (Joosten and Clarke, 2002). Here, in permafrost areas, are found the southernmost lowland periglacial formations of the Northern Hemisphere. They are characterised by the formation of palsa mires (Seppälä, 2011; Sollid and Sørbel, 1998). Palsas are small geomorphological forms composed of an ice core overlain by peat. They form through the cyclical freeze–thaw of water contained in the peat, which causes the permafrost core to expand and the surface to be uplifted (Krüger et al., 2017; Seppälä, 1986). They form in conditions of low snowfall (which allows for deep freezing of the ground in winter) and dry summers (which favour the thermal insulating properties of the peat overlay) (Seppälä, 1986, 2011). The microtopography of palsa mires creates a mosaic of

https://doi.org/10.5194/egusphere-2026-3763
Preprint. Discussion started: 21 July 2026

vegetation and water conditions that differs from more homogeneous low or transitional peatlands (Seppälä, 2011). These differences have significant implications for local ecosystem responses to climate change. That palsa mires occur in permafrost border zones (Leppiniemi et al., 2023) makes them extremely sensitive to climatic fluctuations (Christiansen et al., 2010; Luoto et al., 2004b), and studies from various regions of their occurrence confirm their ongoing degradation due to climate warming (Leppiniemi et al., 2023; Mamet et al., 2017; Olvmo et al., 2020; Verdonen et al., 2023).

Being remote, the changing environmental parameters of northern areas are poorly accessible for in-situ research. This makes them suitable for analysis using satellite remote sensing (RS) (Duncan et al., 2020; Hjort and Luoto, 2006; Sjögersten et al., 2023), which enables continuous and repeatable observations (Wulder et al., 2012). RS is thus an important tool for monitoring environmental changes in permafrost regions (Chen et al., 2022; Jorgenson and Grosse, 2016; Philipp et al., 2021; Wenzl et al., 2024). Such monitoring often employs indirect remote sensing indicators for analysis of changes in vegetation (Crichton et al., 2022, 2025; Yang et al., 2024), water conditions (Li et al., 2024), moisture (Crichton et al., 2025) or surface temperature (Westermann et al., 2011). Studies have indicated that these environmental parameters are being affected by permafrost degradation and active layer deepening (Jin et al., 2022, 2021). Analysis of these parameters therefore supports research on degradation and other changes within permafrost areas (Nitze and Grosse, 2016), which attests to the great importance of research into local environmental conditions for permafrost monitoring (Chadburn et al., 2017). At the same time, researchers emphasise the importance of monitoring permafrost (directly and indirectly), including its response to local and regional climate changes (Hjort et al., 2022), due to the potentially large impact of its thawing on the global climate (Bartsch et al., 2023; Schuur et al., 2015, 2022; Turetsky et al., 2020).

Remote sensing is being applied to an increasing range of types of research in northern areas due to the rapid increase in availability of satellite image data in recent decades (Wulder et al., 2012), including open multispectral data obtained from the Landsat programme (Wulder et al., 2012; Zhu et al., 2019). Landsat satellites, jointly developed by NASA and USGS (Wulder et al., 2019), provide images with a spatial resolution of 30 m and offer a long, continuous series of observations dating back to the 1970s (Anding and Kauth, 1970), as well as a wide spectral range (Wulder et al., 2019). Thanks to the increased availability of satellite data, analyses using these data in studies of permafrost regions have moved from analyses of single-year data to studies using multi-year data series, allowing for continuous monitoring of these areas (e.g., Crichton et al., 2025; Nitze and Grosse, 2016). Satellite data are therefore a valuable source of data for monitoring northern environments (Philipp et al., 2021), including changes in wetlands and peatlands (Abdelmajeed and Juszczak, 2024; Czapiewski and Szumińska, 2022; Demarquet et al., 2023; Ikkala et al., 2026; Zhao et al., 2026).

The aim of the research presented here was to determine the directions of changes in selected environmental parameters of northern Finland in the period 1985–2024 using satellite data from the Landsat programme. The study area is located within the range of sporadic, isolated patches of permafrost (Gisnås et al., 2017), and palsa mires occur within its boundaries (Seppälä, 2006). The study investigated long-term changes in remote sensing indicators describing environmental conditions in a selected area covered by permafrost, with particular emphasis on the dynamics of palsa mires. A secondary objective was to check the suitability of Landsat data for studying long-term changes (40 years). Such a study period is, on the one hand, a challenge due

https://doi.org/10.5194/egusphere-2026-3763
Preprint. Discussion started: 21 July 2026

to the lower availability of satellite images for the 20th century compared to the last two decades. However, on the other, it provides an opportunity to determine the directions of changes resulting from long-term climate change.

The research also analysed the relationship between the calculated remote sensing indicators and selected, relatively constant environmental features, including elevation differences, slope, aspect, and soils, which may influence climatically determined changes in such elements as moisture or vegetation. The analysis included only those environmental parameters that could be clearly identified based on available cartographic databases. In this analysis, particular attention was paid to the potential distinctiveness of palsa mires in relation to other types of peatlands (non-palsa organic soils) and non-peatland areas (mineral soils). This distinction enabled the identification of directions of changes and of the factors determining the dynamics of these climate-change-sensitive forms, which are also indicators of the state of permafrost.

2 Study designs and methods

2.1 Geographical features of study area

The study area covers an area of 402 km^2 (Figure 1A) in northern Finland (Figure 1B), in the catchment area of the Tana River and its right-bank tributary, the Vetsijoki, in a sub-Arctic climate zone (Peel et al., 2007) strongly influenced by both Atlantic and continental circulation. The area is characterised by wet, cool winters and relatively short, cool summers (Autio and Heikkinen, 2002). The study area was selected for its occurrence of palsa mires (0.5% of the area), while excluding areas encompassing deep river valleys (e.g., near the Tana and Usjoki rivers), because the main factor determining environmental conditions in such valleys is relief, which could distort the interpretation of the analysed processes. Furthermore, the study area was selected to fit within one satellite scene.

The study area has a young glacial landscape with elevations ranging approximately from 105 to 445 m above sea level (Figure S1). The dominant features are undulating areas, with the Vetsijoki river valley constituting a central depression and higher elevations to the east and west. The analysis of terrain slopes showed that flat and moderately inclined areas predominate (0–5° over 80% of the study area), whereas areas with significant slopes (>5°) occur locally, mainly in the edge zones of hills (Figure S2). The terrain has a predominantly eastern aspect, while the least common aspect is southern (Figure S3).

The geological structure of the study area is varied. In the southwest, quartz diorite and biotite paragneiss with amphibolite interbeds dominate. From the northwest to southeast, quartz feldspar paragneiss predominates with gabbro and biotite paragneiss interbeds. In the southeast, there is also tonalitic migmatite, while the northeast is occupied by granodiorite with interbeds of ultramafic rock (Figure S4). There are numerous lakes throughout the area, some of which accentuate the deformation zones, but with most being related to ice sheet activity (Tikkanen, 2002). The soil map reveals a predominance of podzols, which are characteristic of northern regions. There are also numerous distric histosols and sapric histosols associated with depressions and shallow initial soils (leptosols) on hills (Figure S5).

In the study area, permafrost currently occurs in the form of isolated patches and sporadic areas (Gisnås et al., 2017). The terrain structure is dominated by open peatlands, especially in the southwest of the study area, with sporadic, sparsely forested

https://doi.org/10.5194/egusphere-2026-3763
Preprint. Discussion started: 21 July 2026

peatlands (Figure S6). Palsa mires also occur in the study area (Figures 1C and S6) (Leppiniemi et al., 2025a, b). Apart from the peatlands, the landscape is dominated by sub-Arctic tundra plant communities (Ahti et al., 1968).

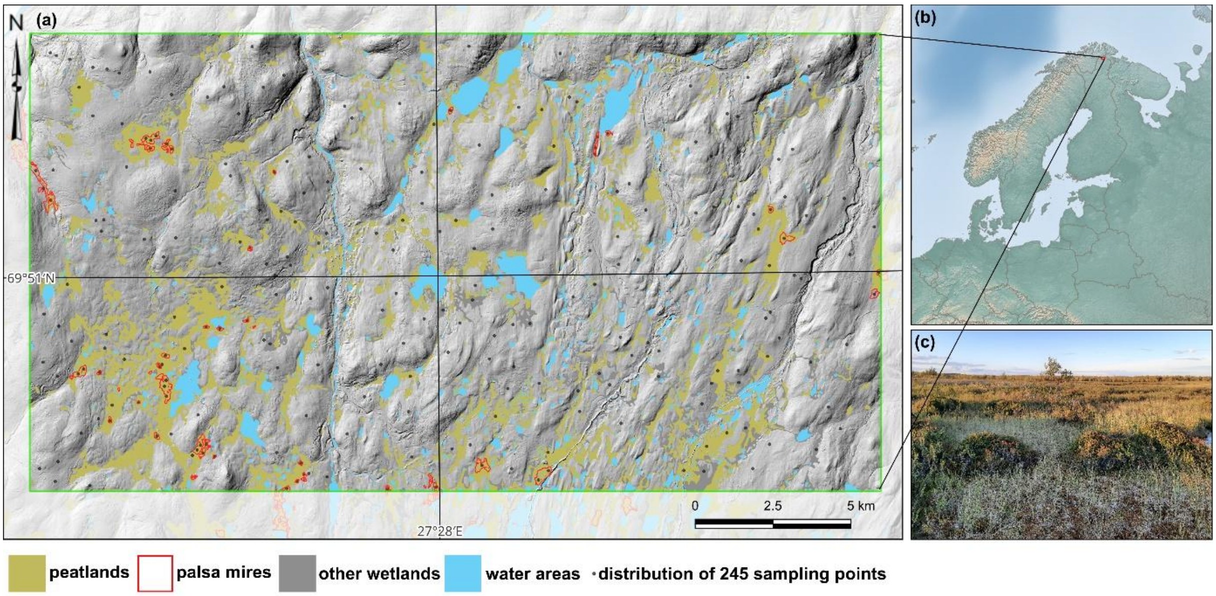

Figure 1. Study area: (a) Location of peatlands, palsa mires and sampling points – points analysed using RS indices on the background of relief and hydrographical network; (b) Location of the research area in Finland; (c) View of the palsa mires in the west site of the study area (photo: August, 2022) (a – prepared based on (National Land Survey of Finland, 2025) and (Finnish Environment Institute (SYKE), 2025), b – prepared based on (Natural Earth, 2026), c – photo by D. Szumińska, August 2022)

2.2 Climate data processing

The analysis of climatic conditions in the study area was performed based on climate data (air temperature, precipitation and snow depth mean) from the Utsjoki-Kevo meteorological station in Northern Finland (~5 km NW of the study area) that were downloaded from the Finnish Meteorological Institute (2025). Those data related to the period 1970–2024, which is 15 years longer than the period analysed based on remote sensing materials (1985–2024). Extending the analysis of climatic conditions to the preceding fifteen years was aimed at providing a more comprehensive understanding of climatic trends in the study area. Based on the obtained data, thermal and precipitation classifications of individual years and months were performed (Tables S5 and S7). Based on the data and the classifications conducted, the course of air temperature and precipitation was analysed, and the trends were calculated using the Mann–Kendall test (PAST 5.2.1. program). All climate data were analysed in terms of annual and monthly values, as well as in terms of three periods selected on the basis of the analysis of air temperature variability (Table S4). Time intervals distinguished based on differences in air temperature conditions (P1: 1985–98; P2: 2000–11 and P3: 2013–24) were used in the RS indicator analyses. The years 1999 and 2012 were omitted from satellite data processing due to the lack of cloudless imagery.

https://doi.org/10.5194/egusphere-2026-3763
Preprint. Discussion started: 21 July 2026

2.3 Remote sensing data processing

The study employed satellite images from the Landsat 5 (TM – Thematic mapper), 7 (ETM+ – Enhanced Thematic Mapper Plus) and 8/9 (OLI – Operational Land Imager) mission satellites with a spatial resolution of 30 m. A flowchart of the satellite data processing and analysis procedure is presented in Figure 2. Cloudless images for the years 1985–2024 were anlysed; they were taken in the morning hours (according to the revisit time of Landsat satellites) in the months June–August (vegetation season, no ice and snow cover). Imagery was downloaded via the USGS EarthExplorer platform (USGS, 2025) and then processed using QGIS 3.36. To ensure data comparability across different sensors, harmonisation based on the methodology of Roy et al. (2016) was used, including correction for spectral differences between generations of Landsat satellites. Values from Landsat 8 OLI were adjusted to be consistent with Landsat 5 TM and Landsat 7 ETM+ using the cross-sensor calibration equations proposed by Roy et al. (2016).

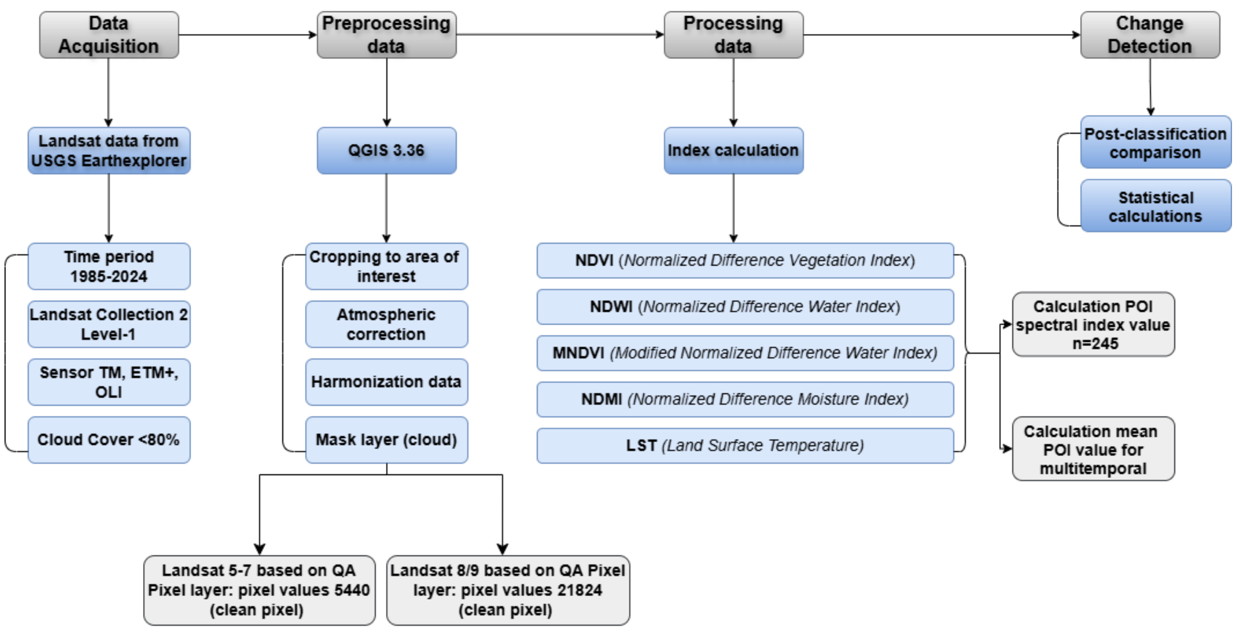

Figure 2. Diagram illustrating the selection process for calculating spectral indices related to environmental changes in northern Finland in the period 1985–2024

The images were generally from the months of June–August, but the dataset also included one image taken on May 31, 2013. Image verification consisted of visual assessment and rejection of data affected by interference, primarily due to cloud cover. Ultimately, images with cloud cover <80% were selected, which meant that no satellite data of adequate quality were available for some years (e.g., 2010, 2015). The selected satellite scenes were then processed in QGIS 3.36 by cropping to the boundaries of the study area and masking clouds. The QA Pixel layer was used to correct the quality of pixels, leaving only the values of

https://doi.org/10.5194/egusphere-2026-3763
Preprint. Discussion started: 21 July 2026

the "clean" pixels for Landsat 5-7 and Landsat 8/9. A total of 58 images (Table S1) that met the criterion of no cloud cover over the study area were used for further analyses.

Based on selected images, the following spectral indices were calculated: NDVI (Normalised Difference Vegetation Index) (Rouse et al., 1974) to assess vegetation changes, NDWI (Normalised Difference Water Index) (McFeeters, 1996) and MNDWI (Modified NDWI) (Xu, 2006) to analyse water conditions, NDMI (Normalised Difference Moisture Index) (Gao, 1996) to determine moisture, and (Land Surface Temperature) (Jimenez and Sobrino, 2003) (Table S2).

The values of remote sensing indices (RS indices) were calculated for 245 sampling points (POI) distributed throughout the study area, covering various substrate types and excluding water areas (lakes and streams and their immediate surroundings) (Figures 1 and S6). About 40% of the sampling points were located on peatlands (96 points; histosols on the soil map) (Figure S5), including palsa mires (48 points). The locations of palsa mires were determined based on Leppiniemi et al. (2025b). Additional points were assigned to mineral soils (149 points). For each point, an average raster value was generated for a buffer size of 60 m (min. 4 pixels). These values were then used to calculate the average values of indices for individual years, the three periods (P1: 1985–98, P2: 2000–11 and P3: 2013–24) and the full study period 1985–2024 (Table S1). The differences between the mean index values for the three time intervals were presented graphically using the generated difference maps. A "decrease" value indicates a >10% decrease in the index value between two periods; likewise, an "increase" value indicates a >10% increase. Additionally, a mosaic of changes was developed by combining the analysis of changes between P1 and P2 and between P2 and P3. Difference maps were not made for LST, because the calculated LST reflects instantaneous thermal conditions (depending, for example, photo acquisition time relative to time of sunrise), while the remaining indices should be considered as representing phenomena that are more stable over time.

2.4 Statistical methods

Remote sensing data were subjected to preliminary data mining using statistical methods (Figures S7-S12). Then, changes in remote sensing indicators and their relationships with environmental features of the study area were analysed using the R environment and the PAST program v.5.2.1 (Hammer et al., 2001), according to the scheme presented in Figure 3.

Pairwise relationships among RS indices were assessed using Spearman rank correlations calculated for point-level mean values. This step examined whether the indices exhibited a common structure of environmental variation and supported subsequent multivariate analyses. Additionally, Spearman rank correlations were computed for environmental variables to evaluate their internal relationships and ensure comparability with the patterns observed in RS-derived indices (Figures S10-S12).

Principal component analysis (PCA) was used to explore the overall covariance structure among indices. PCA was performed on five remote sensing variables (NDVI, NDWI, MNDWI, NDMI, and LST; multi-year means of 245 points) to identify the main environmental gradients in the dataset. The analysis was conducted on z-score standardised data to eliminate the influence of differences in measurement scales. PCA results were visualised using scaling 2 in the vegan package, which emphasises relationships among variables and allows direct interpretation of variable loadings (arrows represent correlations

https://doi.org/10.5194/egusphere-2026-3763
Preprint. Discussion started: 21 July 2026

of variables with the ordination axes). The variable *SOIL_reclass* was not included in the PCA directly and was used solely as a categorical variable for visual classification of points (three groups: 0 – mineral soils; 1 – non-palsa organic soils; 2 – palsa mires).

Due to the hierarchical structure of the data, which includes repeat observations collected at the same sampling points over time, and the lack of statistical independence of measurements, as well as the absence of data for some years, linear mixed-effects models (LMM) were used in the statistical analyses (Pinheiro and Bates, 2000). Moreover, LMMs can properly accommodate unbalanced repeated-measures data, which is the structure of our dataset. In subsequent steps, multivariate statistics were used, based on the average values of RS indices for specific periods or the entire multi-year period.

Firstly, to check for a general temporal trend in each index, separate LMMs were fitted for NDVI, NDWI, MNDWI, NDMI and LST, with year as a fixed effect and sampling point (POINT_FIN) as a random intercept:

$$\text{Index\_value} \sim \text{year} + (1 \mid \text{POINT\_FIN})$$

Year was treated as a continuous predictor and centred prior to analysis. Models were fitted using restricted maximum likelihood (REML), and the estimated slope for year, its 95% confidence interval, associated p-value, and marginal and conditional R2 values were reported. Marginal R2 represents the proportion of variance explained by year alone, and conditional R2 represents the proportion explained by the full model, including both the fixed effect and random differences among sampling points.

Further, to test whether the RS indices differed among the three soil categories (mineral soils, non-palsa organic soils, and palsa mires) and whether their temporal trajectories differed, separate mixed-effects models were fitted with year, soil category, their interaction as fixed effects, and POINT_FIN as a random intercept:

$$\text{Index\_value} \sim \text{year} \times \text{soil category} + (1 \mid \text{POINT\_FIN})$$

Significant effects were followed by post-hoc pairwise comparisons of estimated marginal means and estimated temporal slopes, with Tukey-adjusted p-values.

https://doi.org/10.5194/egusphere-2026-3763
Preprint. Discussion started: 21 July 2026

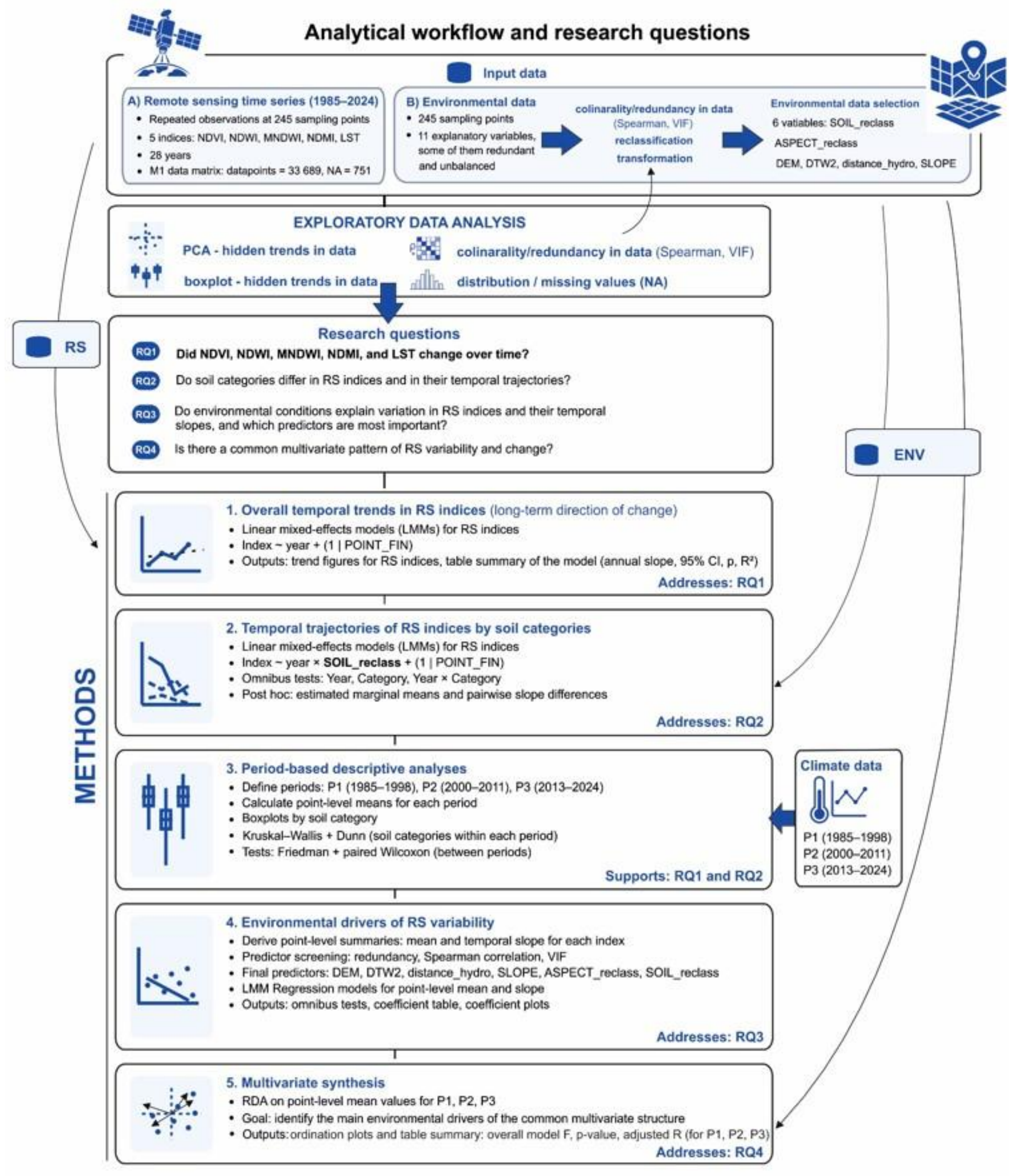

Figure 3. The statistical calculation process

https://doi.org/10.5194/egusphere-2026-3763
Preprint. Discussion started: 21 July 2026

To examine environmental controls of remote sensing indices variability, point-specific mean values and temporal slopes were calculated for each RS index and used as response variables in regression models with environmental predictors representing topography, hydrology and soil.

Continuous predictors were standardised, categorical predictors were treated as factors, and predictor redundancy was assessed using Spearman correlations and variance inflation factor (VIF) at the initial data exploration step (Figures S10-S12). All mixed-effect linear models analyses were performed in R (R Core Team., 2025) using the packages lme4 (Bates et al., 2015), lmerTest (Kuznetsova et al., 2017) and emmeans (Lenth et al., 2026).

Then, Redundancy Analysis (RDA) was performed for the selected independent variables (environmental parameters) and all remote sensing indicators (dependent variables). This analysis was applied to test whether environmental predictors explained the shared multivariate structure of the RS signal. The analysis included environmental characteristics related to: terrain elevation (DEM), exposure (ASPECT), slope (SLOPE), groundwater depth (DTW2), soil category (SOIL_RECLASS) and distance from the nearest water body or watercourse (distance_hyro) (Table S3). These were assigned in the database to each of the 245 points based on the source materials presented in Supplementary Material (Figures S1-S6). The input data were standardised z-scores within the dependent and independent variable matrix. Both multivatiate analysis (PCA and RDA) were performed with the vegan package (Oksanen et al., 2022).

Furthermore, boxplots were used as a complementary tool to visualise the distribution and variability of RS indices across predefined study periods and soil categories. Their role was to illustrate temporal structure, capturing phase-specific differences and between-group contrasts, thereby supporting the interpretation of mixed-effects analyses.

3 Results

3.1 Factor analysis of RS indices

In the analysis of correlations between satellite indices, the strongest negative relationship was between NDVI and NDWI (r=-0.97), which indicates that high surface water content in the study area accompanies low vegetation intensity. This indicates the presence of wetlands, peatlands and water bodies with limited vegetation cover. In turn, NDVI and NDMI show a strong positive correlation (r=0.84), confirming their utility for assessing the condition and water content of vegetation. Being based on difference between NIR and SWIR bands, NDMI well reflects moisture changes in plant biomass, as reflected in its consistency with NDVI. The high, negative correlation between NDVI and surface temperature LST (r=-0.66) indicates the cooling effect of more heavily vegetated areas. This phenomenon is due to the effect of transpiration and shading, which lower ground temperatures in heavily overgrown areas. Additionally, water and moisture indices were each noted to correlate strongly negatively with LST (LST/MNDWI: r=-0.68; LST/NDMI: r=-0.76) (Figure S12).

The correlation analysis indicates diverse connections between environmental parameters and RS indices. The strongest positive relationship (r=0.7) is between the terrain slope (SLOPE) and the Cartographic Depth to Water Index (DTW2) parameter. In turn, DTW2 also shows a moderate positive correlation with distance from watercourses (distance_hydro) at the

https://doi.org/10.5194/egusphere-2026-3763
Preprint. Discussion started: 21 July 2026

level of 0.41. The strongest negative correlations were recorded for the ASPECT_reclass feature in relation to slope (SLOPE, r=-0.55) and DTW2 (r=-0.39). The DEM (elevation) variable is most weakly related to the remaining predictors, with correlation coefficients not exceeding the absolute value of 0.25 (Figure S10). The strongest positive correlations were found between LST and DTW2 (r=0.63) and between LST and slope (r=0.55) (Figure S11). NDVI correlates moderately negatively with DEM (r=-0.45) and DTW2 (r=- 0.44), which suggests higher plant productivity in depressions and with higher soil moisture. NDMI has its strongest negative correlation with DTW2 (r=-0.45, this also being DTW2's strongest negative correlation), followed by SLOPE (r=-0.42) and DEM (r=-0.41), confirming the importance of terrain relief in the concentration of surface moisture. In general, moisture-related indices (NDMI and MNDWI) are closely related to hydrological conditions (DTW2), which indicates their sensitivity to the local retention capacity of the substrate. In turn, the relationship between LST and DTW2 constitutes the strongest positive correlation for both indices (r=0.63). Thus, though surface temperature is conditioned by meteorological conditions, it is also determined more strongly by water conditions than any other index studied here and can also influence substrate moisture (Figure S11).

The PCA conducted for RS indices revealed a strong underlying structure in the remote sensing dataset. The first principal component (PC1) explains 75.7% of the total variance, while the second (PC2) accounts for 16.1%. Together, the first two components explain over 91% of the total variability, indicating an efficient dimensionality reduction (Figures 4a-c).

Table 1. Loadings of the first five principal components (PC1–PC5) obtained from Principal Component Analysis (PCA) of remote sensing variables (NDVI, NDWI, MNDWI, NDMI, and LST; multi-year means). Loadings indicated the contribution of each variable to the respective principal components

Index	PC 1	PC 2	PC 3	PC 4	PC 5
MEAN_NDVI	0.9073	-0.4043	-0.0295	0.1120	-3.34E-05
MEAN_NDWI	-0.8892	0.4265	-0.1438	0.0811	0.0111
MEAN_MNDWI	0.7415	0.6380	0.2052	0.0307	-0.0107
MEAN_NDMI	0.9734	0.1176	0.1933	-0.0308	0.0186
MEAN_LST	-0.8195	-0.1935	0.5387	0.0272	0.0004

The loadings indicate that PC1 is primarily associated with vegetation and moisture indices (NDVI, NDMI – rather than temperature and water-related variables [LST, NDWI]), which represent the main environmental gradient. PC2 reflects a clear contrast between water presence (MNDWI, NDWI) and vegetation (NDVI) (Table 1). The distribution of soil categories (SOIL_reclass) in the PC1–PC2 space (Figure 4a) exhibits a clear relationship with the identified environmental gradients. Palsa mires (SOIL_reclass=2) and other organic soils (SOIL_reclass=1) located along higher PC1 values are associated with increased vegetation and moisture (NDVI, NDMI), whereas mineral soils (SOIL_reclass=0) at lower PC1 values correspond to higher surface temperatures (LST) and reduced moisture conditions (MEAN_NDWI). Along PC2, there is no clear separation of soil categories (Figure 4a). The clear separation of points in the ordination space indicates that the analysed soil

https://doi.org/10.5194/egusphere-2026-3763
Preprint. Discussion started: 21 July 2026

categories have unique and measurable remote sensing signatures. Soil categories (SOIL_reclass) show a clear and ordered distribution along the main environmental gradient (PC1), indicating a strong relationship between soil type and vegetation–moisture conditions. Soils on mineral substrates are associated with warmer and drier conditions, whereas organic soils (palsa and non-palsa mires) correspond to more vegetated and moist conditions (Figure 4a).

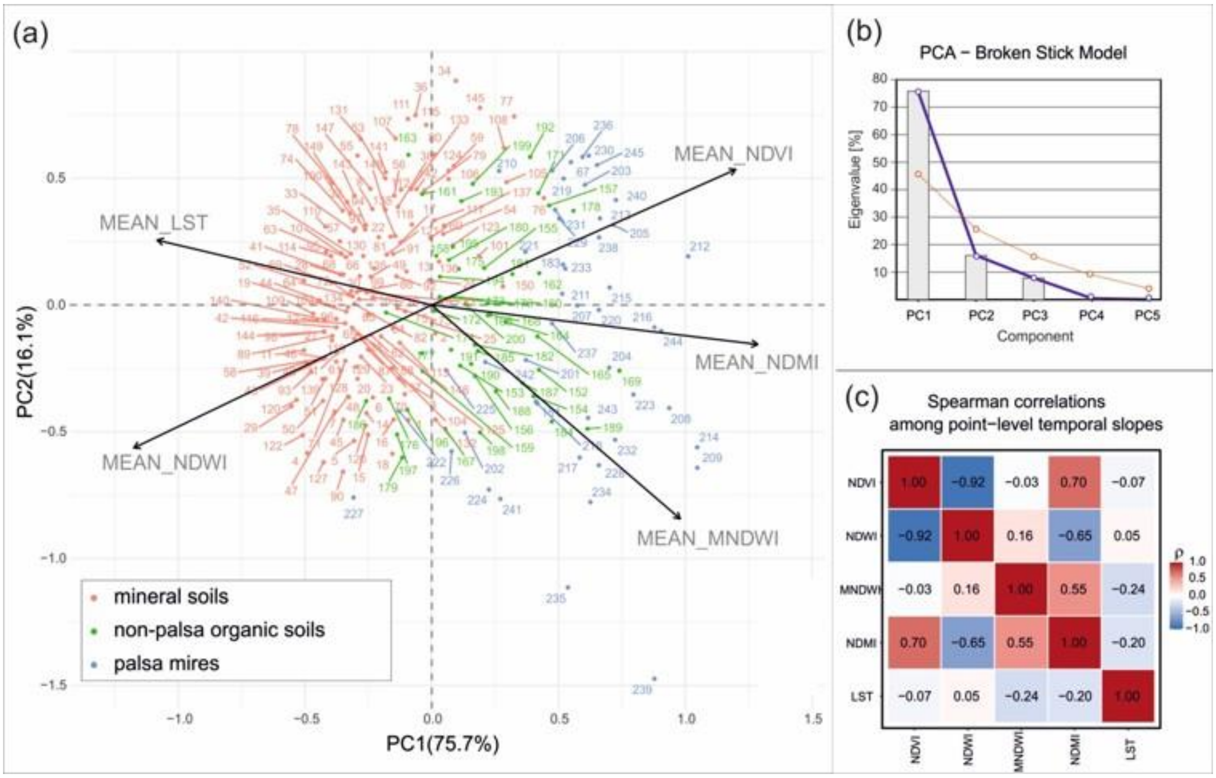

Figure 4. (a) Principal Component Analysis (PCA) biplot of remote sensing variables: NDVI, NDWI, MNDWI, NDMI, and LST; multi-year means (calculated based on Landsat data (USGS, 2025)) (b) Broken stick model (c) Correlation Spearman's rs of the average values of remote sensing indices

3.2 Temporal changes of air temperature and precipitation

In the study period (1985–2024), the multi-year mean annual air temperature calculated for the Utsjoki-Kevo station was -0.8 °C, while the multi-year mean annual precipitation reached 426 mm (Table S4). In the full meteorological period 1970–2024, a statistically significant upward trend in mean air temperatures of ~0.42 °C per decade was observed (Z=4.20, p=0.00003) (Figure S13). A similarly statistically significant (Z=3.29, p=0.00099) upward trend of 0.52 °C per decade occurred for the period 1985–2024. Among the summer months analysed based on satellite scenes, July was the warmest, with a multi-year average air temperature of 13.5 °C (Figure S14 and Table S4). During the period 1985–2024, years were classified from anomalously cold to very warm, with 15 normal years, 18 warm to very warm years, and only 7 cool to anomalously cool years. The year 2024 was very warm, and 1985 was anomalously cold (Table S6).

Atmospheric precipitation showed a slight, statistically insignificant, upward trend in the years studied, of the order of 0.9 mm per year. In turn, linear regression analysis indicates a decreasing number of precipitation days of ~1–1.5 days per year (Figure S15). During the period under review, years ranged from very dry to very moist, with 16 normal years, 9 moist, 6 very moist, 8 dry, and 1 very dry (1990) (Table S8). Detailed air temperature and precipitation characteristics for individual months of the study period are presented in Supplementary Material.

Linear regression analysis showed a significant decreasing trend in the number of snow cover days between 1975 and 2024, averaging ~0.65 days per year (R^2=0.449). In terms of snow cover depth, no clear time trend was observed, as confirmed by the very low coefficient of determination (R^2<0.001). The results indicate a shortening of snow persistence with a simultaneous high variability of average cover thickness (Figure S16).

The analysis of air temperature changes at the Utsjoki Kevo station (Figure S13) allowed three different periods to be identified. The first (P1: 1985–98) is characterised by high interannual variability of air temperature and lower mean annual air temperature, as compared to the later years. The average temperature for the period was -1.5 °C, and the average annual temperature was lowest in 1985 (-3.6 °C) and highest in 1989 (0.3 °C) (Table S4). The average annual rainfall for this period was 425 mm. The second period (P2: 2000–11) is characterised by a greater amplitude of air temperature variability and more frequent occurrence of mean annual temperatures exceeding -1 °C. The mean temperature for the period was -0.5 °C, and the mean annual temperature was lowest in 2010 (-2.1 °C) and highest in 2011 (0.6 °C). The average long-term annual rainfall for the period was 433 mm. In the most recent period (P3: 2013–24), there is less year-to-year variability in mean annual air temperature and a greater frequency of mean annual temperatures exceeding -0.5 °C or even 0 °C. This period is clearly warmer than periods P1 and P2, with a mean temperature of -0.1 °C. The lowest average annual temperature occurred in 2019 (-1.4 °C) and the highest in 2024 (0.9 °C). The long-term average annual rainfall during this period was 402 mm (Table S4).

3.3 Temporal variation and trends of remote sensing indices

Linear mixed-effects models revealed significant temporal trends for all analysed RS indices over the study period 1985–2024. NDVI and NDMI showed positive trends, indicating an overall increase in vegetation greenness and moisture-related conditions. In contrast, NDWI and LST exhibited significant negative trends, while MNDWI showed a weak but statistically significant positive trend (Figure 5).

The strongest positive temporal trends were found for NDMI, followed by NDVI (Table 2). NDWI decreased significantly over time, and LST also showed a negative trend. Although MNDWI increased significantly, this effect was small. The marginal R2 values were generally low to moderate, indicating that time alone explained only a limited proportion of the total variance, whereas the substantially higher conditional R2 values suggest that a considerable part of the variability was associated with persistent differences among sampling points (Figure 5, Table 2).

https://doi.org/10.5194/egusphere-2026-3763
Preprint. Discussion started: 21 July 2026

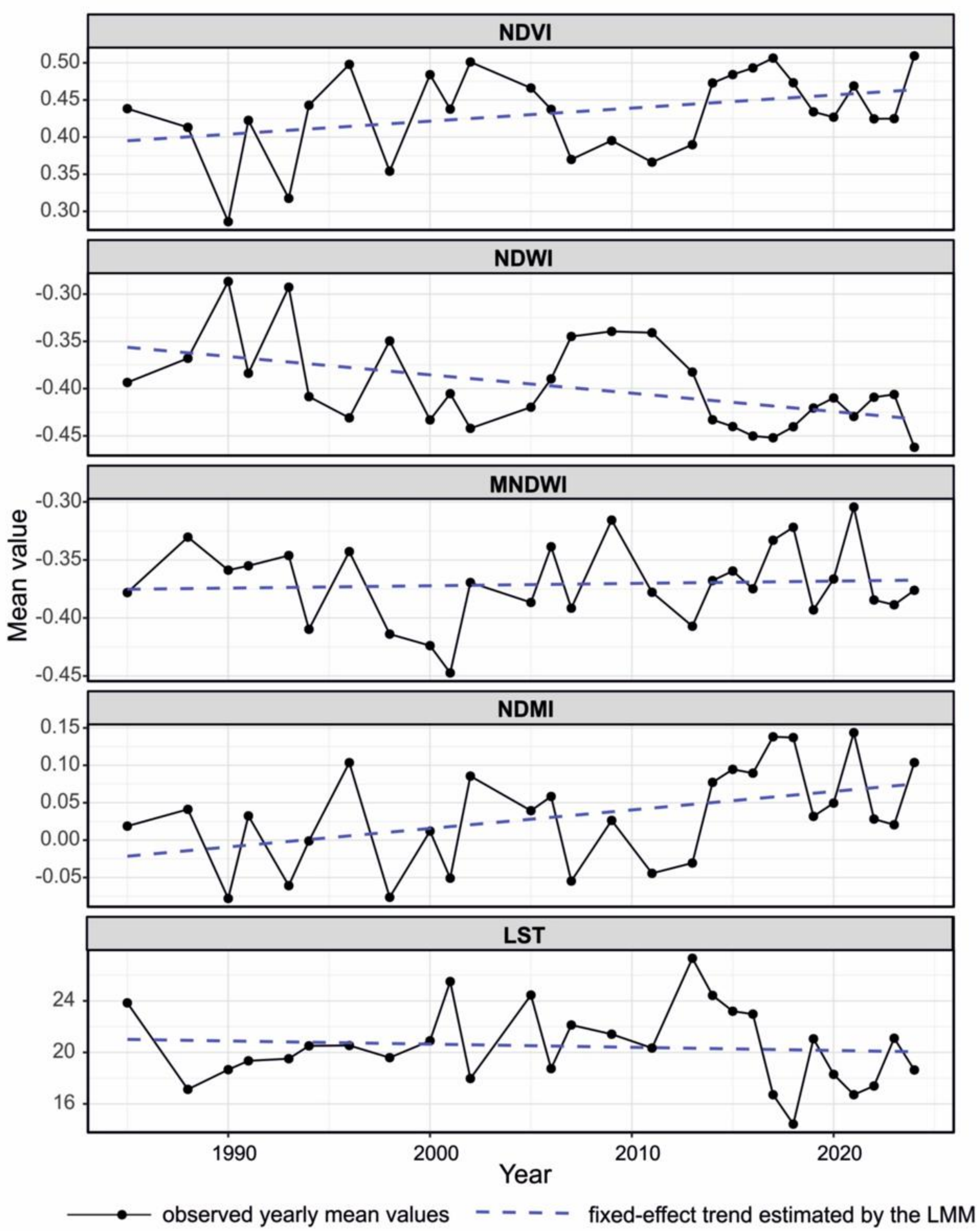

Figure 5. Temporal changes of NDVI, NDWI, MNDWI, NDMI, and LST across the study period (1985–2024) (calculated based on Landsat data (USGS, 2025))

https://doi.org/10.5194/egusphere-2026-3763
Preprint. Discussion started: 21 July 2026

Table 2. Results of linear mixed-effects models testing temporal trends in remote sensing indices across the study period (1985-2024) (calculated based on Landsat data (USGS, 2025)).

Index	Trend (β/year)	95% CI	p-value	Marginal R^2	Conditional R^2
NDVI	0.0018	0.0016, 0.0019	<0.001	0.068	0.406
NDWI	-0.0019	-0.0020, -0.0018	<0.001	0.12	0.498
MNDWI	0.0002	0.0001, 0.0003	<0.001	0.001	0.482
NDMI	0.0025	0.0023, 0.0026	<0.001	0.068	0.611
LST	-0.0246	-0.0310, -0.0182	<0.001	0.006	0.301

The variability of satellite indicators based on the 245 points distributed over the study area showed differences depending on point locations. Points located on palsa mires exhibited greater amplitudes of fluctuations in of most remote sensing indices (NDVI, NDWI, NDMI, MNDWI) (Figures 6 and S17). The exception was the LST index, which in the areas of palsa mires and other organic soils had significantly (~4 °C) lower and less diverse values compared to points in areas outside peatlands (i.e., in those with mineral soils). The two organic categories did not differ significantly from each other (Figure 6 and Table S9). At the same time, the points located on palsa mires stood out for having the lowest spatial variation in surface temperature. Importantly, palsa mires exhibited higher NDVI, MNDWI and NDMI values and lower NDWI values compared to the other sites; NDWI, in contrast, reached their highest level on mineral soils (non-peatland) (Figure 6 and Table S10).

Pairwise comparisons were conducted to further investigate the significant main and interaction effects detected in the mixed-effects models (Table 3). The comparisons showed a clear and consistent gradient for NDVI, MNDWI and NDMI, with their values being highest in palsa mires, intermediate in other organic soils, and lowest in mineral soils. Differences in temporal trajectories were most evident for NDVI and NDMI, with mineral soils showing weaker positive trends than both categories of organic soils. For NDWI, mineral soils showed a weaker negative trend than other organic soils and palsa mires. In contrast, no significant pairwise differences in slope were detected for MNDWI, and only weak evidence of slope differences was found for LST (Figure 6 and Table S9).

https://doi.org/10.5194/egusphere-2026-3763
Preprint. Discussion started: 21 July 2026

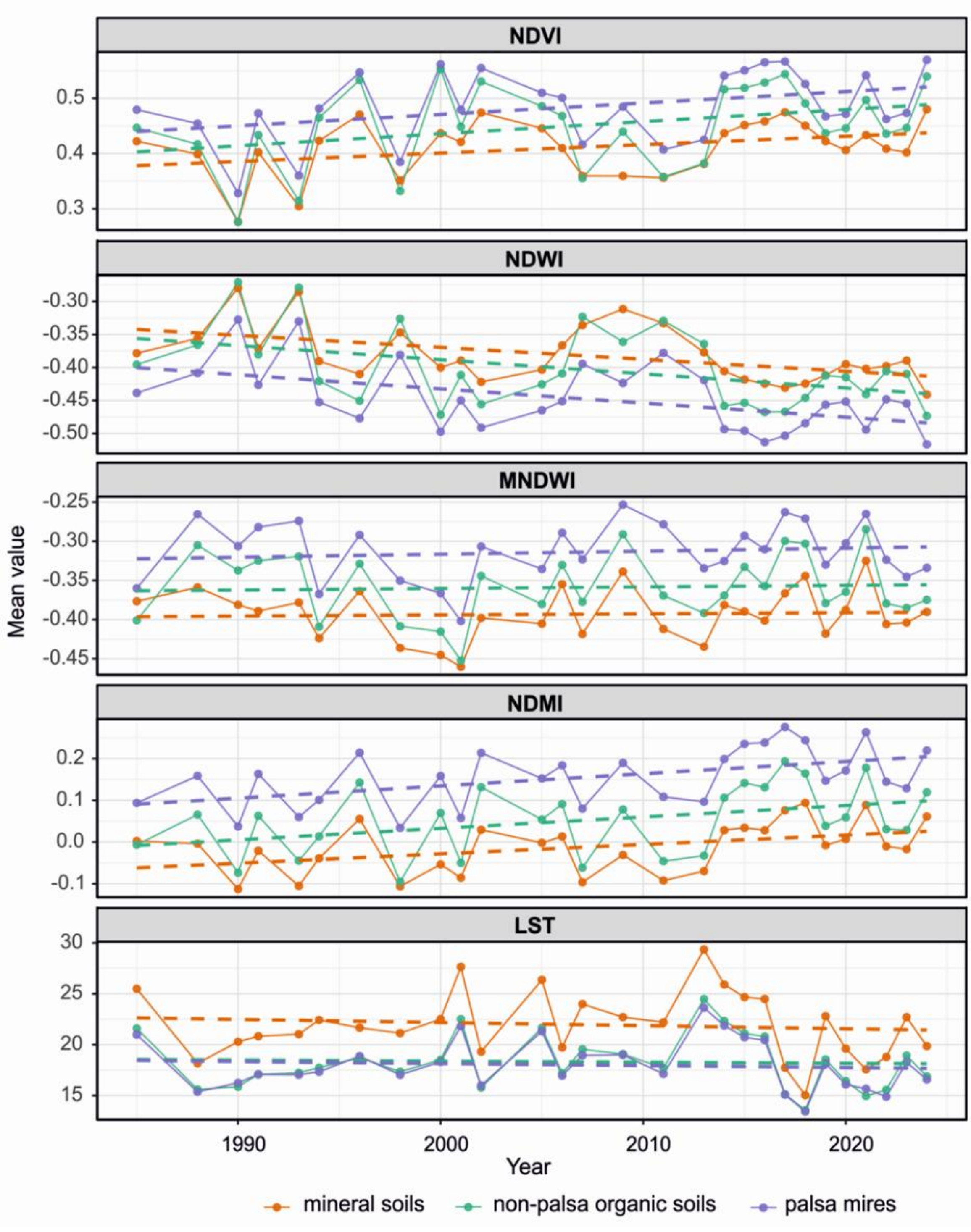

325 **Figure 6.** Temporal changes of NDVI, NDWI, MNDWI, NDMI, and LST across the study period (1985–2024) in the three soil categories (calculated based on Landsat data (USGS, 2025))

https://doi.org/10.5194/egusphere-2026-3763
Preprint. Discussion started: 21 July 2026

Table 3. Summary of mixed-effects models testing the effects of soil category on remote sensing indices and their temporal trajectories.

	Year		Soil category		Year × soil category	
Index	**F**	**p**	**F**	**p**	**F**	**p**
NDVI	F(1, 6465.0) = 704.11	< 0.001	F(2, 242.1) = 79.77	< 0.001	F(2, 6465.0) = 11.12	< 0.001
NDWI	F(1, 6464.6) = 1332.42	< 0.001	F(2, 242.0) = 72.43	< 0.001	F(2, 6464.6) = 5.54	0.004
MNDWI	F(1, 6461.8) = 19.74	< 0.001	F(2, 242.2) = 114.86	< 0.001	F(2, 6461.8) = 1.91	0.148
NDMI	F(1, 6462.5) = 1012.71	< 0.001	F(2, 241.9) = 199.56	< 0.001	F(2, 6462.5) = 8.15	< 0.001
LST	F(1, 6461.9) = 29.30	< 0.001	F(2, 243.1) = 389.92	< 0.001	F(2, 6461.8) = 2.99	0.050

***F**, omnibus test statistic, **Adjusted p** indicates the p-value corrected for multiple comparisons; values < **0.05** were considered statistically significant*

Within analysis of the three study periods (P1: 1985–88, P2 2000–11, P3: 2013–24), soil categories differed significantly for all analysed indices (all Kruskal–Wallis tests: $p<0.001$; Table 11). Post-hoc Dunn tests showed that NDMI and MNDWI consistently distinguished all three categories in every period, and the same overall pattern was observed for NDVI. For NDWI, all three categories differed significantly in P2 and P3, whereas in P1 the contrast between mineral soils and non-palsa organic soils was not significant. For LST, mineral soils differed significantly from the organic soil categories (both palsa and other) in all periods, while non-palsa organic soils and palsa mires did not differ significantly from each other (Tables S11 and S12).

The average index values for periods P1, P2 and P3, calculated for points grouped by soil category, indicate clear changes over time. They also confirm the previously indicated variability in these changes among mineral soils, non-palsa organic soils, and palsa mires (Figures 7 and S18). The vegetation index (NDVI) clearly increases through P1, P2 and P3 for all soil categories, and the median NDVI in each period is notably higher for palsa mires (0.46–0.52) than for other organic soils (0.40–0.48) or mineral soils (0.37–0.43) (Figures 7 and S18). This indicates that biomass productivity is highest within palsa mires. There is a similar increase through P1, P2 and P3 for the soil moisture index (NDMI) in all soil categories, with the increase being most pronounced between periods P2 and P3. Median water indices for all soil categories either decreased across P1, P2 and P3 (NDWI) or decreased between P1 and P2 then increased between P2 and P3 (MNDWI). In P1, the average air temperature was -1.5 °C, followed by -0.5 °C and -0.1 °C in P2 and P3, respectively (Table S4), indicating a persistent climate warming trend in the study area. Bearing in mind that LST is the most temporally variable of the studied indices, the median of this index was notably lowest at points representing all soil categories in P1, then increased in period P2 and decreased slightly in period P3. Treating the set of indices as comprehensive information about the environment, the decrease in LST in P3 may result from increased moisture (increases in NDMI and MNDWI), which may have changed the radiation balance of the land surface. Considering the slight (~5–7%) decrease in atmospheric precipitation in P3 compared to P1 and

https://doi.org/10.5194/egusphere-2026-3763
Preprint. Discussion started: 21 July 2026

P2 (Table S4) and the constant upward trend in air temperatures, the increase in area humidity in the summer months may have been contributed to by ice degradation within the palsa mires. At the same time, the persistent decrease in median NDWI and accompanying increases in NDMI and MNDWI suggest a tendency for changes towards wetland conditions rather than an increased number and area of water bodies. Notably, the P3 period, especially its second half, was characterised by exceptionally warm, dry months in June–August on a multi-annual scale (Tables S6 and S8), which may have resulted in large water losses to evaporation and transpiration. It is also noteworthy that, as shown earlier, palsa mires differ clearly in the values of the analysed indices, not only from mineral soils, but also from other organic soils (Figure 7); they constitute sites with higher plant productivity, higher moisture and lower surface temperature.

The spatial differentiation of environmental dynamics in the study area in the study period is presented on maps of differences in remote sensing index values among the three sub-periods (Figures S19-S22). NDVI increased between P1 and P2 across the vast majority (61%) of the study area, but there was no change between P2 and P3 (in 95% of total area) (Figure S19). However, there is an increase in NDVI between both P1 and P2 and P2 and P3 within peatlands and along streams and in the vicinity of water bodies, which indicates highly dynamic hydrological processes and the associated variability of vegetation. Stable areas (unchanged) occur mainly in areas above 300 m a.s.l. that are characterised by slopes of <15° (Figures S1, S2 and S19).

For the NDMI moisture index, most of the area exhibited either no change between P1 and P2 (85% of total area) and an increase between P2 and P3 (61% of total area) or no change between P1 and P2 nor between P2 and P3 (24% of total area) (Figure S20). In P1–P2, increases in NDMI were recorded mainly along watercourses, in the vicinity of lakes, and on peatlands, while the index remained unchanged in the rest of the area. Between P2 and P3, conditions were stable in areas surrounding rivers and lakes, whereas values continued to increase within palsa mires. The most stable moisture conditions are found on the slopes of larger valleys and depressions (slopes of >5°; Figures S2 and S20).

The MNDWI index was highly stable in most of the study area (no index changes in 81% of total area) (Figure S21). In P1–P2, decreases were only local, whereas in P2–P3 local increases occurred. The NDWI index exhibited clear temporal and spatial variability. In P1–P2, it decreased in 37% of the study area (Figure S22). In P2–P3, decreases of >10% occurred mainly in and around peatlands, while the index value was stable elsewhere. Importantly, within a few hundred metres of the dynamically changing peatlands, no significant changes were recorded, which emphasises the point-specific nature of the NDWI index values.

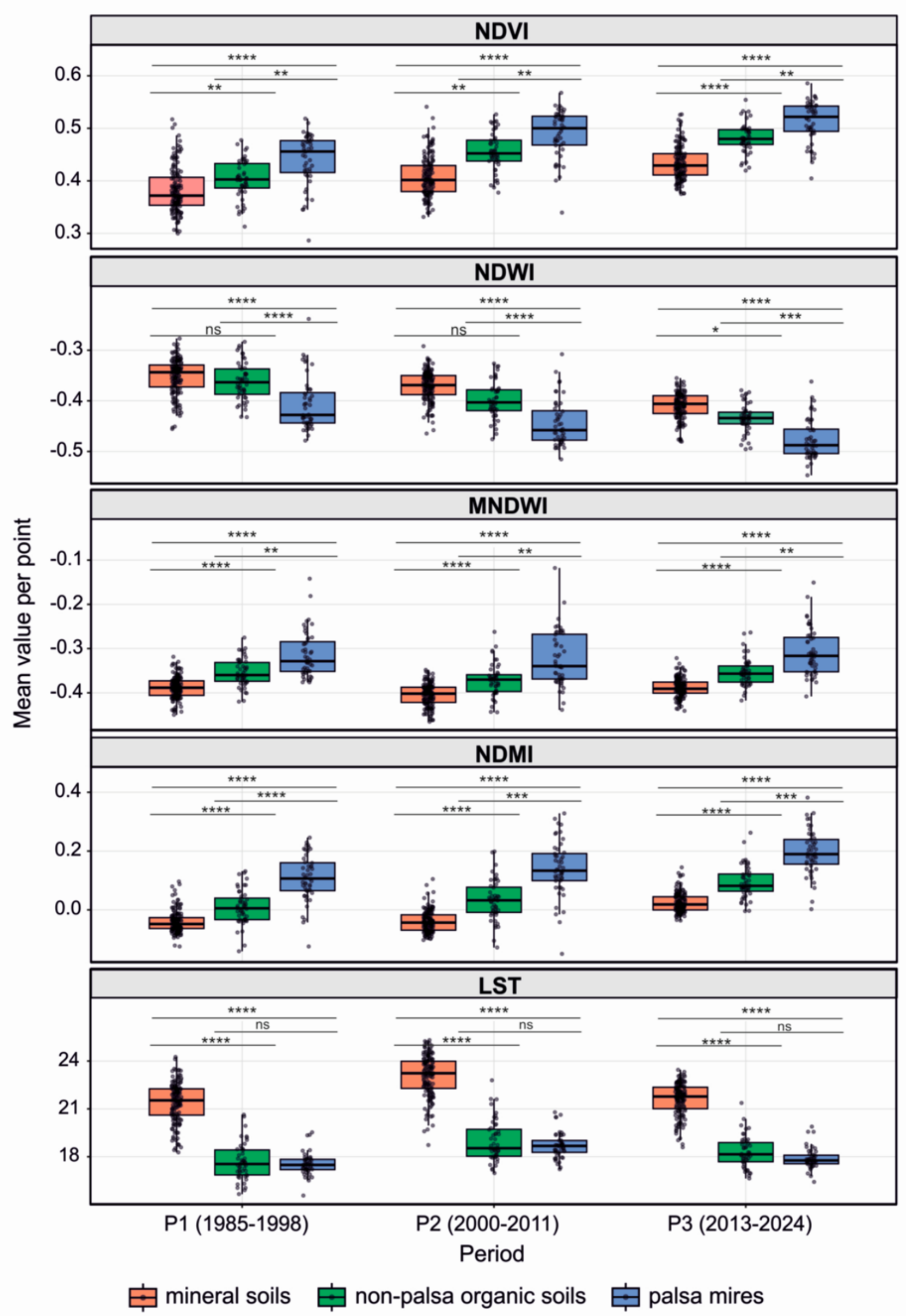

380 **Figure 7.** Distribution of point-level mean values of NDVI, NDWI, MNDWI, NDMI, and LST across three study periods (P1, P2, P3), shown separately for soil categories (calculated based on Landsat data (USGS, 2025)). Asterisks above comparisons indicate statistical significance from Dunn post-hoc tests: * p<0.05, ** p<0.01, *** p<0.001, **** p<0.0001, ns = not significant.

https://doi.org/10.5194/egusphere-2026-3763
Preprint. Discussion started: 21 July 2026

3.4 Environmental drivers of remote sensing variability

Omnibus tests showed that soil category was the most consistent predictor of remote sensing variability, significantly explaining the point-level mean values of all five indices and the temporal slopes of all indices except MNDWI. DEM was the second most important predictor, with significant effects on the mean values of NDVI, NDWI, NDMI and LST and on the temporal slopes of the same indices. In contrast, DTW2 was significant only for mean LST, whereas distance to hydrographic features and slope did not show significant effects in the final models. Aspect had a more selective influence, significantly affecting mean LST and the temporal slopes of NDVI and LST (Tables 4 and S13).

The coefficient estimates further indicated that, relative to mineral soils, both palsa mires and other organic soils were associated with higher mean values of NDVI, NDMI and MNDWI and with lower mean values of NDWI and LST. For temporal slopes, soil category was again important: compared with mineral soils, organic soils generally showed stronger positive trends in NDVI and NDMI and more negative trends in NDWI. DEM also showed a coherent pattern, being negatively associated with the mean values of NDVI and NDMI, positively associated with mean NDWI and LST, and significantly related to the temporal slopes of these indices (Figure 8 and Table S13).

Table 4. Omnibus tests of environmental predictors for point-level mean values and temporal slopes of remote sensing indices: A – Models for point-level mean values, B – Models for point-level temporal slopes

A												
Index	**DEM**		**DTW2**		**Distance hydro**		**Slope**		**Aspect**		**Soil category**	
	F	**p-value**	**F**	**p**	**F**	**p-value**	**F**	**p-value**	**F**	**p-value**	**F**	**p-value**
NDVI	32.33	<0.001	2.87	0.091	0.01	0.94	3.64	0.058	0	0.986	38.48	<0.001
NDWI	19.22	<0.001	1.61	0.206	0.02	0.879	1.36	0.245	0.85	0.356	32.47	<0.001
MNDWI	1.25	0.264	1.6	0.207	0.31	0.58	0.08	0.775	0.11	0.741	56.99	<0.001
NDMI	15.74	<0.001	0	0.951	0.16	0.688	0.55	0.458	0.14	0.705	95.62	<0.001
LST	6.24	0.013	4.13	0.043	0.55	0.458	0.12	0.732	4.72	0.031	200.21	<0.001
B												
Index	**DEM**		**DTW2**		**Distance hydro**		**Slope**		**Aspect**		**Soil category**	
	F	**p-value**	**F**	**p-value**	**F**	**p-value**	**F**	**p-value**	**F**	**p-value**	**F**	**p-value**
NDVI	53.53	<0.001	0.23	0.628	3.51	0.062	1.17	0.281	7.57	0.006	18.03	<0.001
NDWI	51.62	<0.001	0.01	0.921	3.44	0.065	0.01	0.917	1.45	0.23	6.78	0.001
MNDWI	0.48	0.49	1.01	0.316	0.09	0.76	0.12	0.725	0.44	0.509	2.59	0.077
NDMI	28.33	<0.001	1.39	0.24	0.58	0.447	0.01	0.912	3.4	0.066	10.55	<0.001
LST	15.48	<0.001	1.6	0.207	0.83	0.364	0.1	0.752	6.38	0.012	11.66	<0.001

Continuous predictors (DEM, DTW2, distance to hydrographic features, slope, and transformed aspect) were standardised before modelling. Soil category was entered as a factor; omnibus tests evaluate the overall effect of the three soil categories. Point-level means were calculated across the full study period, and slopes were estimated from linear regressions of each index against centred year for each sampling point. p-values <0.05 were considered statistically significant.

https://doi.org/10.5194/egusphere-2026-3763
Preprint. Discussion started: 21 July 2026

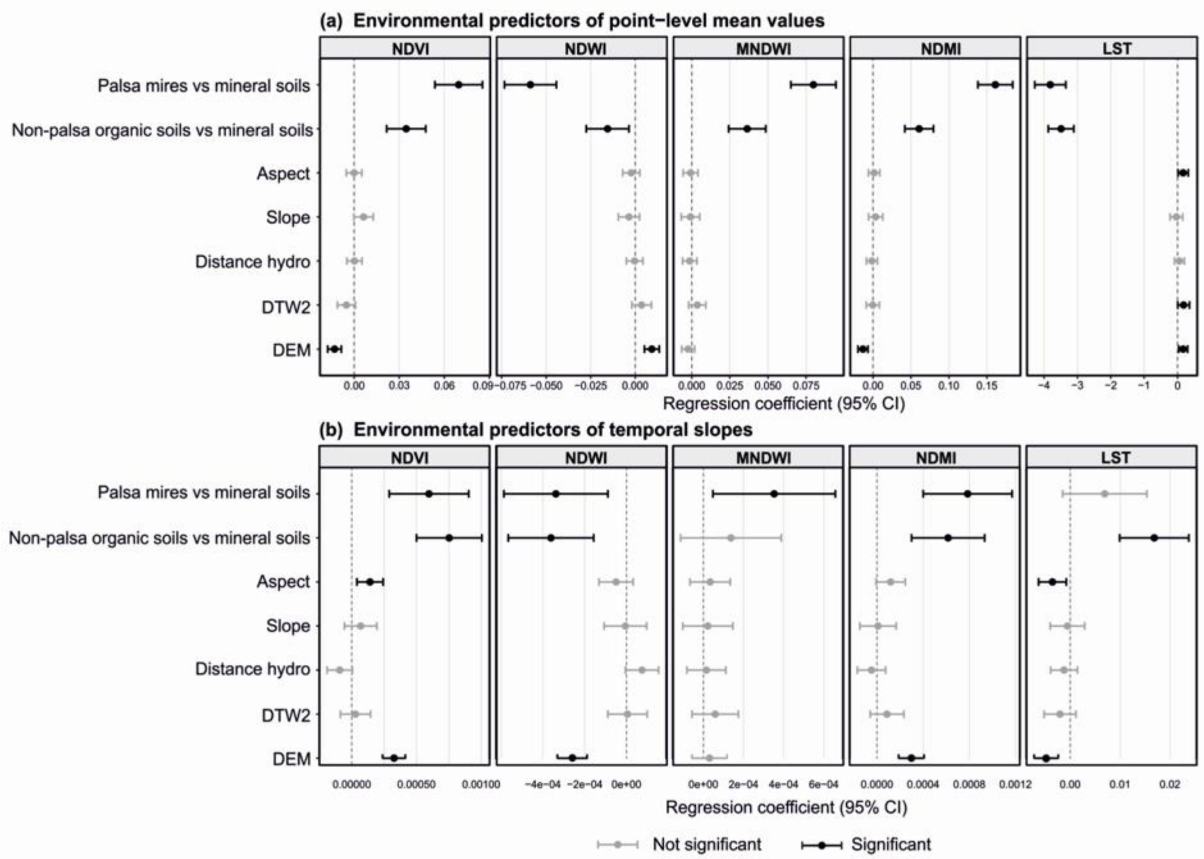

Figure 8. Coefficient plot showing regression estimates and 95% confidence intervals for: (a) environmental predictors of point-level mean values and (b) temporal slopes of NDVI, NDWI, MNDWI, NDMI and LST (Continuous predictors aspect, slope, distance_hydro, DTW2 and DEM were standardised, and coefficients for soil category are expressed relative to mineral soils)

Redundancy analysis (RDA) showed that environmental predictors significantly explained the shared multivariate structure of remote sensing indices in all three study periods. The overall constrained models were highly significant in P1, P2 and P3 (all $p=0.001$), indicating that the joint variation in standardised point-level mean values of RS indices was strongly structured by environmental conditions. The explanatory power of the models was substantial and increased slightly over time, with adjusted R2 values of 0.496 in P1, 0.544 in P2, and 0.586 in P3 (Tables 5, S14 and S15). In all three periods, the first constrained axis dominated the ordination, accounting for 89.9% of the constrained variance in P1, 93.9% in P2 and 95.2% in P3, whereas the second axis explained only a small additional proportion (7.8%, 4.1% and 3.5%, respectively; Table 5). This indicates that the environmentally structured component of RS variability was organised mainly along a single dominant gradient.

https://doi.org/10.5194/egusphere-2026-3763
Preprint. Discussion started: 21 July 2026

Table 5. Summary of redundancy analysis (RDA) models across the three study periods.

Period	Overall model F	p-value	Adjusted R²	RDA1 (%)	RDA2 (%)
P1	34.57	0.001	0.496	89.9	7.8
P2	42.15	0.001	0.544	93.9	4.1
P3	50.15	0.001	0.586	95.2	3.5

Overall model significance (F) is based on permutation tests. Adjusted R^2 values indicate the proportion of multivariate variation in standardised point-level mean remote sensing indices explained by the constrained model within each period.

The distribution of points in the RDA biplots (Figure 9) indicates partial clustering of objects. Soil category (SOIL_reclass) clearly separates the studied points into three groups, suggesting that this environmental variable and satellite indicators significantly differentiate the studied area internally. Permutation tests for individual predictors showed that soil category, DTW2 and DEM were the strongest and most consistent drivers of the multivariate RS structure across all three periods (Table S13). Soil category was highly significant in P1, P2 and P3, and its contribution increased toward the most recent period. DTW2 was also strongly significant throughout and became particularly important in P3, whereas DEM showed a stable and substantial effect across all periods. Distance to hydrographic features and slope were consistently significant but clearly weaker, while aspect had the weakest and least stable influence. The ordination plots supported this interpretation by showing a clear environmental structuring of the multivariate RS space (Figure 9). Sampling points belonging to different soil categories occupied distinct positions in the ordination space, and the main RS indices were aligned along the dominant constrained gradient. Together, these results indicate that the joint RS signal was not random, instead being strongly organised by substrate-related, hydrological and topographic conditions, with this environmental control remaining robust across all three temporal phases.

https://doi.org/10.5194/egusphere-2026-3763
Preprint. Discussion started: 21 July 2026

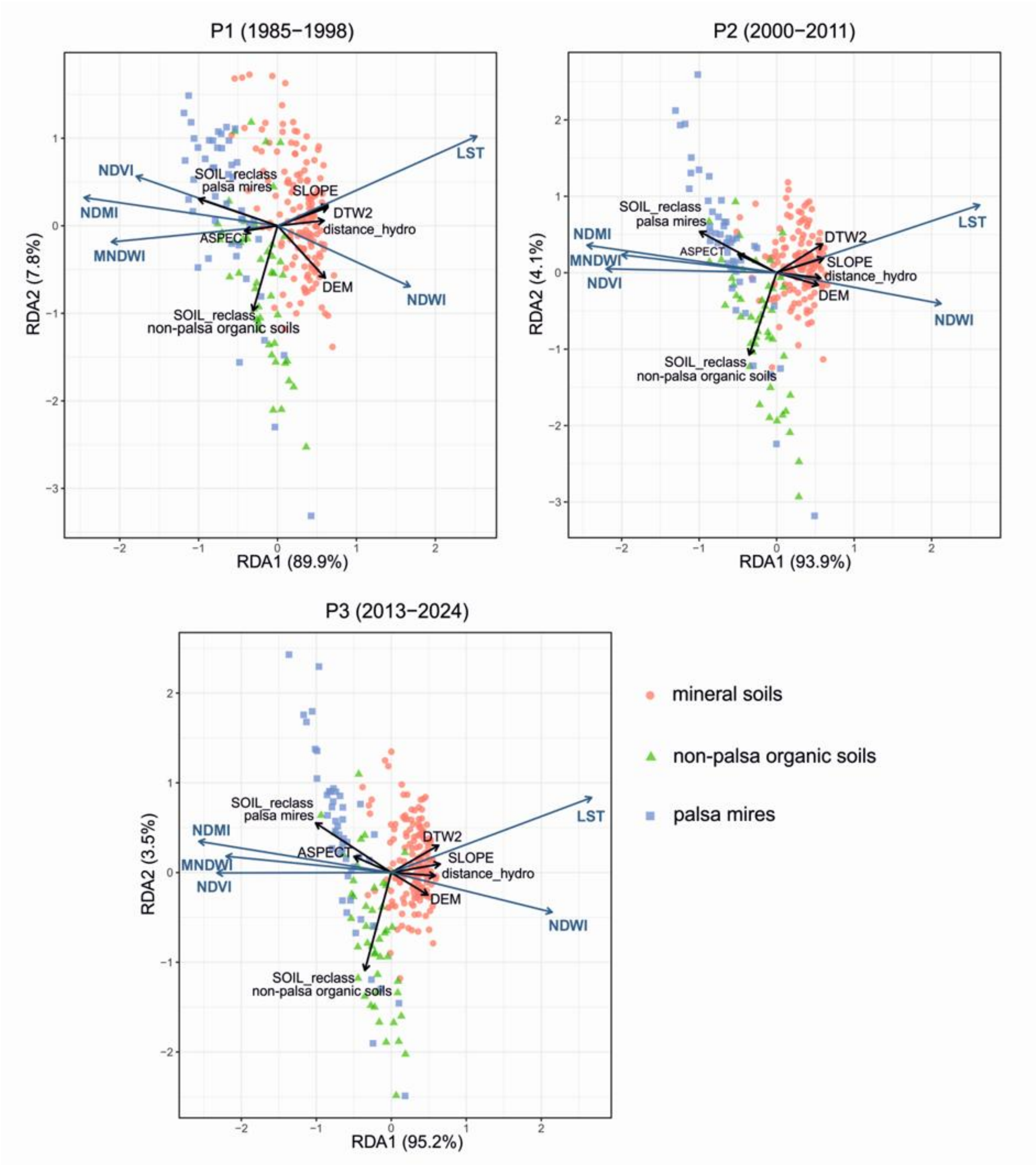

Figure 9. RDA biplots of standardised point-level mean RS (NDVI, NDWI, MNDWI, NDMI) values for P1, P2 and P3 periods according to soil reclassification groups (calculated based on Landsat data (USGS, 2025))

https://doi.org/10.5194/egusphere-2026-3763
Preprint. Discussion started: 21 July 2026

4 Discussion

Permafrost, especially discontinuous permafrost, is susceptible to the rapid climate warming that has been observed in the Arctic in recent decades (Schuur et al., 2008). According to recent studies, the temperature increase in permafrost regions is almost four times faster (3.8 °C between 1979 and 2021) than in the rest of the globe (Rantanen et al., 2022), and this trend is steadily continuing (Biskaborn et al., 2019; Smith et al., 2022). Permafrost degradation causes greenhouse gases to be released into the atmosphere (Hugelius et al., 2020; Turetsky et al., 2020), which further exacerbates warming and, as a result, progressively reduces the extent of permanently frozen ground (Schuur et al., 2015, 2022). The degree of permafrost degradation varies significantly across areas, which may result partly from differences in climatic conditions and vegetation cover (Streletskiy et al., 2015).

4.1 Interrelationships between satellite indicators and environmental factors

The relationships between remotely sensed indicators and environmental parameters reveal a spatial variability in ecosystem response to climate warming in northern Finland. The observed increase in NDVI and NDMI, together with the decrease in LST, suggests that the study area underwent a directional environmental change consistent with increasing vegetation-related and moisture-related signals and reduced surface thermal load. However, these patterns should be interpreted cautiously, as remote sensing indices represent indirect proxies of environmental processes and may also be influenced by image-acquisition timing, sensor-specific characteristics, and short-term weather variability (Pettorelli et al., 2014). The weak but significant trend in MNDWI indicates that not all water-related indices responded equally strongly, which may reflect differences in their environmental sensitivity and interpretability (Xu, 2006).

PCA analysis showed a clear differences in the distribution of points according to substrate type, demonstrating that substrate type strongly determines environmental conditions and spectral signals. The main factor controlling the variability of Landsat indices in the study area is the gradient in the variation in moisture conditions and vegetation cover. The dominance of NDVI and NDMI within PC1 indicates an increase in plant productivity and surface moisture. The pattern of LST and NDWI in areas outside peatlands being opposite to that of NDVI and NDMI may indicate colder conditions in waterlogged areas.

The RDA results extend the index-specific regression models (LMM) by showing that environmental predictors structured the remote sensing system at a multivariate level, rather than influencing only individual indices in isolation. Whereas the regression models identified which variables were associated with the mean values and temporal slopes of particular indices, RDA demonstrated that a large proportion of the shared variation among NDVI, NDWI, MNDWI, NDMI, and LST was jointly organised by environmental conditions. This methodological complementarity aligns with observations by Álvarez-Martínez et al. (2026), who noted that, although univariate models successfully capture high-frequency, short-term environmental dynamics, a multivariate ordination is essential to synthesise stable, spatial topographic–soil gradients. In particular, soil category (mineral soils, non-palsa organic soils, and palsa mires), DTW2 and DEM emerged as the strongest

https://doi.org/10.5194/egusphere-2026-3763
Preprint. Discussion started: 21 July 2026

and most consistent predictors of the common RS structure across all three periods. The permanence of these predictors is rooted in the physical mechanisms governing the sub-Arctic landscape; mineral soils facilitate high thermal conductivity and lower moisture, which accelerates summer thaw and increases ground temperatures, whereas the organic peat layers of palsa mires act as a powerful thermal insulator (Muir et al., 2025). This indicates that the observed RS patterns were not simply a set of separate index-specific responses, but instead reflected an integrated environmental gradient linking substrate conditions and hydrological and topographic setting. Specifically, the high stability of the DTW index underscores its capacity to model water table positions and soil drainage zones (Larson et al., 2022; Murphy et al., 2009), which directly dictate physiological vegetation stress, translating into a tightly coupled response of moisture (MNDWI, NDMI) and vegetation (NDVI) indices. Thus, RDA provided an important synthetic perspective, confirming that environmental control operated not only at the level of single indicators, but also at the level of the overall multivariate RS signal.

4.2 Temporal changes of remote sensing indices

The analysis of the Landsat mission time series revealed significant environmental changes in the studied part of northern Finland (Figures 1 and S19-S22). The RS indices calculated based on Landsat data (such as NDVI, NDWI, NDMI) in this work have already been successfully used to monitor environmental changes on a temporal scale in northern regions (e.g., Chen et al., 2022; Liu et al., 2025; Nitze et al., 2018; Nitze and Grosse, 2016). The analysis of three time periods (P1: 1985–98, P2: 2000–11, P3: 2013–24) indicated a gradual but clear trend, which can be interpreted as a transition from a more stable environment characterised by the occurrence of permafrost to systems dominated by peat-forming and hydrological processes.

The increase in NDVI in the periods P1–P3 may indicate intensifying “Arctic greening”, i.e. an increase in vegetation productivity under warming climate conditions (Berner et al., 2020; Myers-Smith et al., 2020). Important findings include that the overall increase in NDVI values in the study during the study period is in line with the commonly observed Arctic greening trend (Yang et al., 2024), which in recent decades amounted to ~1.8% per decade (Seo and Kim, 2024). The increase in vegetation productivity in this region is usually associated with increased average air temperatures and a longer growing season (Myers-Smith et al., 2020). Shijin and Xiaoqing (2023) and Yang et al. (2024) showed that the increase in NDVI in Arctic regions intensifies with increasing active-layer thickness, and that the main determining factor is permafrost degradation.

At the same time, our study found an increase in NDMI, which is a strong indicator of water content in plant tissues (Gao, 1996). Combined with increasing MNDWI values, which reflect open water and ground saturation (Xu, 2006), this indicates an increase in moisture content of both the surface layer and vegetation. This trend supports the hypothesis that northern permafrost areas are transforming into more water-rich ecosystems, where depressions associated with permafrost degradation and plant expansion result in the pixel containing more water “in vegetation”. Thus, NDVI showed a high positive correlation with NDMI (0.84; Figure S12) indicating the relationship between vegetation productivity and moisture. This relationship is characteristic of wetland and tundra areas, where vegetation development is strongly controlled by hydrological conditions and the active soil layer (Loranty et al., 2011).

https://doi.org/10.5194/egusphere-2026-3763
Preprint. Discussion started: 21 July 2026

In turn, the decrease in NDWI found in the study may have been strongly disturbed by the development of dense vegetation, especially in peatlands during the growing season. In such conditions, the signal reflected from plants dominates in the water signal, thus limiting the index's ability to detect ground moisture and possibly producing underestimated values despite high ground moisture. MNDWI is more effective at detecting open water in complex landscapes, especially where vegetation and moist soils are present, whereas NDWI may be more sensitive to changes in "water pixels" (Zhou et al., 2017). Giese et al. (2025) pointed out that, on a European scale, there is a clear rising trend in moisture content (rising NDMI) in peatland areas in the boreal part of the continent, although locally it is shaped by high heterogeneity of hydrological conditions (a larger number of small wet spots, less water area), which confirms our results.

LST values in Arctic regions are strongly determined by surface properties such as moisture, vegetation cover or permafrost condition (Westermann et al., 2011), and studies on tundra energy balances indicate that any change in the insulating properties of vegetation and soils directly modifies the surface temperature (Helbig et al., 2020; Langer et al., 2010). Despite the increase in air temperature recorded by the meteorological station, remote sensing analysis showed a local downward trend in LST in our study area that was particularly pronounced within the peatlands. This discrepancy indicates that surface temperature in peatland ecosystems is not only determined by the direct influence of air temperature but also by local hydrological conditions and changes in vegetation structure. These values may also be related to changes in the energy balance structure, which increases latent heat flux at the expense of sensible heat, leading to effective surface cooling (Nedbal et al., 2020), even when the region as a whole experiences long-term warming (Worrall et al., 2019). The spatial thermal variability of the tundra can be captured using Landsat data, which enable high-resolution estimations of energy balance components (Nedbal et al., 2020). The strong negative correlation found between LST and NDVI, NDMI and MNDWI indices ($r \approx -70$, Figure S12) proves that hydrological processes are effectively limiting the impact of regional warming in the study area.

It should be noted, however, that the LST value does not directly reflect long-term air temperature trends (recorded by the weather station). While the stations record continuous changes in air temperature (24 hours a day), LST represents the surface state only at the specific moment of the satellite's overflight and is strongly dependent on atmospheric conditions and data acquisition time, and its analysis is based on a limited number of observations per month (e.g., 1 or 2 scenes available per month). Consequently, LST is highly susceptible to short-term atmospheric conditions and daily variability. In contrast, vegetation and water/moisture indices (e.g., NDVI, NDMI) reflect the integrated vegetation/moisture response over the entire growing season. Their values result from the cumulative impact of environmental conditions (temperature, moisture, water availability) and not from the conditions prevailing on a single day. For this reason, discrepancies between the indicator values obtained do not necessarily indicate a contradiction, but may instead result from differences in time scales and in the nature of the indicators.

https://doi.org/10.5194/egusphere-2026-3763
Preprint. Discussion started: 21 July 2026

4.3 Changes of environmental characteristics of the palsa mires

The results obtained for the studied part of northern Finland, which lies at the marginal extent of permafrost occurrence and features palsa mires (Seppälä, 2006), indicate differences in the thermal and hydrological character of palsa mires in the boreal zone as compared to the remaining peatlands and other soil types in this area (represented mainly by podzols). Palsa mires constitute a specific type of peatlands associated with the presence of permafrost, and their functioning depends heavily on the relationship between thermal and hydrological conditions (Seppälä, 2011). The analysis of 45 points located on palsa mires showed them to be characterised by higher soil moisture and lower and more stable surface temperature, as compared to mineral soils and non-palsa organic soils. This is due to the presence of permafrost and ice in the peat profile (Seppälä, 2011), which cushions seasonal thermal fluctuations and limits infiltration (Kujala et al., 2008). Increased surface moisture favours an energy balance shift towards the latent heat flux (Helbig et al., 2020), which limits surface heating and may locally decrease LST.

In the study area, the highest NDVI values were recorded on palsa mires rather than at points located on other peatlands or outside them. The analysis of trends over time (40 years: 1985–2024) showed an increase in NDVI in P3 compared to the earlier periods P1 and P2, suggesting a slight increase in plant productivity in the study period. Bosiö et al. (2012) analysed palsa mires in Fennoscandia and indicated that climate changes within them were leading to the transformation of plant communities and an increase in the share of plants preferring more humid habitat conditions. This trend is confirmed by studies of “Arctic greening”, which is being observed in many high-latitude regions (Heijmans et al., 2022; Myers-Smith et al., 2020).

In the study period, an upward trend was observed that was similar for the NDMI and MNDWI indices. It was seen at sites represented by the 245 points (Figure S18) as well as across the area as a whole (Figures S20 and S21). The results indicate a progressive increase in environmental moisture and vegetation development related to the degradation of permafrost and hydrological changes occurring within palsa mires. Previous studies have shown that ice loss within palsa mires increases substrate moisture (Laurent et al., 2025), as reflected in high values of satellite indices reflecting moisture (NDMI and MNDWI). Similar spectral changes were reported by Kolari et al. (2022), although their study concerned a boreal aapa mire rather than a palsa mire. Using Landsat data from 1985–2020, they showed that increasing NIR reflectance, together with increasing GDVI and decreasing AWEI, was associated with the replacement of formerly open, wet flark surfaces by Sphagnum carpets and lawns. Their findings therefore support the interpretation that changes in moisture dependent peatland vegetation and surface wetness can strongly affect satellite derived spectral indices (Kolari et al., 2022). Furthermore, a study that included areas of northern Finland (around Kevo), Crichton et al. (2025) found a consistent increase in NDVI on more than two thirds of analyse peatland edges (over the last 15–20 years) with stable or increasing moisture (NDMI).

A different situation was observed for the NDWI index, which showed a decrease in value in the analysed period. As described in section 4.2, this may suggest a reduction in surface water availability or changes in vegetation structure affecting the spectral response of the indicator. The indicator NDWI is traditionally applied to delineate open water features (McFeeters, 1996), while MNDWI more accurately reflects both open water bodies and zones of high soil-moisture saturation (Xu, 2006).

https://doi.org/10.5194/egusphere-2026-3763
Preprint. Discussion started: 21 July 2026

As a result, a concurrent rise in MNDWI coupled with a decline in NDWI may indicate progressive wetting of the ground within palsa mires. The expansion of water-saturated surfaces increases MNDWI, whereas permafrost degradation and the resulting vegetation development increase NIR reflectance, thereby decreasing NDWI. It is also interesting that NDWI values were lowest on palsa mires as compared to the other substrate types, which may be due to their unique relief. Their ice core elevates these formations above the mire level, which forces a natural slope of the terrain. As a result, water does not accumulate on the tops of the palsas but flows down to the lower depressions.

The results obtained can be associated with the specificity of the study area, and specifically with the presence of palsa mires that are subject to strong degradation (Leppiniemi et al., 2025b; Luoto et al., 2004a). Studies monitoring the state of these forms indicate their successive reduction in the Northern Hemisphere (Aalto et al., 2017; Borge et al., 2017; Fewster et al., 2022; Mamet et al., 2017; Olvmo et al., 2020). In Fennoscandia, bioclimatic models indicate that, by the end of the 21st century, climatic conditions throughout the region will no longer be conducive to maintaining permafrost and its associated palsa mires (Fewster et al., 2022; Fronzek et al., 2006; Leppiniemi et al., 2023). In contrast, forecast models indicate an almost complete loss of environmental conditions suited to palsa mires in the Northern Hemisphere by 2061–80, under a high-emission scenario (RCP8.5), but even under moderate and low-emission scenarios the projected loss is 89.3% and 76.3%, respectively (Leppiniemi et al., 2023). For example, detailed studies of two palsa mires in the Kilpisjärvi area (Finland) showed their areas to have decreased by 77–90% and their heights by 16–49% between 1959 and 2021 (Verdonen et al., 2023), which indicates intensive permafrost degradation. This process is closely related to the spatial variation of active layer thickness (ALT), which is greatest at the edges of the forms, leading to their erosion (Verdonen et al., 2024). Moreover, recent studies indicate that 53% of palsas in northern Finland are in poor morphological condition and only 28% have maintained good ecological status (Leppiniemi et al., 2025b).

Previous studies show that, in the past, climate warming led to increased carbon accumulation in high-latitude peatlands (Gallego-Sala et al., 2018; Piilo et al., 2020). However, contemporary warming is bringing about more diverse responses in permafrost-associated peatlands, which results from dynamic hydrological and ecological changes (Sim et al., 2021). Models indicate that Arctic peatlands will remain a carbon sink in the coming decades (northern peatlands will become a CO2 source of ~0.2 Pg C year-1 by 2300 under RCP8.5) (Qiu et al., 2022), but around the mid-21st century they may become a carbon source due to drying, permafrost thawing and vegetation changes (Gallego-Sala et al., 2018). Moreover, a possible disturbing effect of palsa degradation is changes in hydrochemical characteristics, including metals accumulated in palsa mires being released into surface waters (Jóźwik et al., 2025).

Considering the environmental changes being seen, further disappearance of palsa mires in the future may gradually transform into boreal peatlands and/or more hydrated communities related to the development of thermokarst and the expansion of water surfaces. However, the thinness of permafrost within the marginal zone of its extent, together with rising air temperatures and the expansion of vegetation (increased evaporation and transpiration), accompanied by no significant upward trend in total precipitation, appears not to favour the increasing extent of open waters that has been observed in regions of continuous and discontinuous permafrost (Jones et al., 2011). At the same time, the environmental response of the palsa

https://doi.org/10.5194/egusphere-2026-3763
Preprint. Discussion started: 21 July 2026

mires of the study area to the increase in air temperatures results from their marginal character; the observed changes, such as changes in hydrological condition (Jin et al., 2022; Liljedahl et al., 2016), are a signal of the palsas' gradual disappearance in this region. At the same time, the results indicate that the rate of permafrost degradation may be spatially diversified due to the heterogeneity of thermal and hydrological conditions – especially in relation to the distance from the hydrographic network, but also other environmental factors, including the height above sea level.

Perspectives of remote sensing study

The results are important due to the need for local research in Arctic regions that has been indicated in the literature (Leppiniemi et al., 2025a; Nitze and Grosse, 2016). This will improve understanding of the potential directions of environmental transformations in the 21st century. The results also indicate the effectiveness of RS detection of changes in moisture, temperature and vegetation at high spatial resolution (30×30 m per pixel) for long time series (1985–2024). The increasing availability of satellite data (e.g., new Copernicus Sentinel earth observation missions), as well as the increasingly rapid development of open source software (e.g., QGIS, SAGA GIS and ESA SNAP), together create promising prospects for using RS data for detailed analysis of changes in environmental components in remote northern areas. Moreover, structured monitoring of permafrost areas can enrich national and international peatland ecosystem observation programmes (e.g., Global Terrestrial Network for Permafrost (GTN-P), Copernicus). Another key perspective for the development of modern remote sensing is the rapid progress in artificial intelligence, with particular emphasis on machine and deep learning algorithms, which are revolutionising data processing and automatic detection of environmental changes (Shang et al., 2026; Zhu et al., 2017).

Limitations due to remote sensing data

Satellite data from the Landsat series play a key role in environmental research, ecosystem monitoring and land cover change analyses at local and global scales (Wulder et al., 2019). Their application is somewhat hampered by atmospheric influences on data quality (Song et al., 2001). The presence of clouds, aerosols and variability of atmospheric conditions can significantly reduce the number of usable scenes, especially in polar regions (Ju and Roy, 2008). Landsat 8 exhibits specific trends for latitudes between 55 and 82 degrees, where data availability is reduced by frequent cloud cover (Rahimi and Jung, 2024). Moreover, the temporal resolution of 16 days for a single satellite, or even 8 days for Landsat 8 and 9 combined, may be insufficient to track acute or extreme processes, such as rapid changes in soil moisture (Roy et al., 2014). In our case, only 58 satellite images from the years 1985–2024 were used due to limitations resulting from cloud cover. At the same time, scenes were most abundant for the last 5 years (2020–24), which creates a risk of uneven data abundance in the time series. It is also important to note that seasonal differences and satellite pass dates can significantly affect spectral indices – comparing images from different days during the season can lead to the false appearance of trends.

https://doi.org/10.5194/egusphere-2026-3763
Preprint. Discussion started: 21 July 2026

5 Summary and conclusions

Satellite images from the Landsat mission were used to calculate selected remote sensing indices for the period 1985–2024, in an area of 402 km^2 within the range of permafrost occurrence in northern Finland. Long-term monitoring encompassing a wide range of spatial and temporal data enabled a comprehensive analysis of changes in the environment of the study area. The trends of the calculated indices (NDVI, NDWI, MNDWI, NDMI and LST) revealed environmental changes over time.

The most important findings are:

1. Temporal trends in the vegetation index (NDVI) and moisture indices (NDMI, MNDWI) increased throughout the entire study period, in contrast to the water index (NDWI) and surface temperature (LST), which decreased towards the end of the study period.
2. A strong positive correlation between the vegetation index (NDVI) and the moisture index (NDMI) was found and a negative correlation between the vegetation index (NDVI) and the water index (NDWI).
3. Spatial differentiations in individual indices and in trends over the period 1985–2024 were found.
4. Discrepancies were found between the air temperature trend (continuous increase) and the surface temperature index trend (decrease at the end of the period).

Clear environmental factors were detected that determined the multidimensional structure of remote sensing indices. Of these, soil categories, DTW2 and DEM were the strongest and most consistent predictors in all three subperiods of 1985–2024. The importance of soil categories and the DTW2 parameter increased significantly in the last period (P3: 2013–24), indicating the progressive intensification of environmental control over the spectral signal. These results also confirmed the clear thermal and hydrological distinctiveness of palsa mires, which throughout the study period retained an environmental character that was entirely distinct from the other organic soils (i.e., dystric histosols, sapric histosols) and the mineral soils (dystric leptosols, endogleyic podzols, hypersceletic leptosols).

The use of Landsat images, being characterised by high spatial resolution (30 metres), enabled the detection of even small spatial changes, which is important due to the heterogeneous and mosaic landscape of the young glacial landscape of northern Finland. At the same time, the Landsat mission provides a long time series of images, which allowed for the analysis of changes over as much as 40 years. The approach used can be easily applied to other study sites, which can help understand and quantify changes in dynamically changing permafrost areas, including those at the margins of its range.

Code and data availability

Detailed values of RS indices calculated for each point was presented in Szczepańska et al. (2026). Dataset for: The use of remote sensing for studying environmental changes in a palsa mire zone of Northern Finland in the period 1985-2024. https://doi.org/10.5281/zenodo.20817134.

Author contributions

MSZ: Conceptualisation, Investigation, Data curation, Formal analysis, Methodology, Validation, Visualisation, Writing – original draft, Writing – review & editing. **SC**: Conceptualisation, Investigation, Data curation, Formal analysis, Methodology, Validation, Visualisation, Supervision, Writing – review & editing. **MS**: Conceptualisation, Formal analysis, Methodology, Validation, Visualisation, Supervision, Writing – original draft, Writing – review & editing. **DS**: Conceptualisation, Investigation, Data curation, Methodology, Validation, Project administration, Resources, Funding acquisition, Supervision, Writing – review & editing.

Competing interests

The authors declare that they have no known competing financial interests or personal relationships that could have appeared to influence the work reported in this paper.

Disclaimer

Copernicus Publications remains neutral with regard to jurisdictional claims made in the text, published maps, institutional affiliations, or any other geographical representation in this paper. While Copernicus Publications makes every effort to include appropriate place names, the final responsibility lies with the authors. Views expressed in the text are those of the authors and do not necessarily reflect the views of the publisher.

Acknowledgements

The authors would like to thank Zakhar Bachkou for helping to download satellite data.

Financial support

This research was funded by the National Science Centre of Poland, PER2 Water project no. NCN 2021/41/B/ST10/02947. The research was also funded by the project Supporting Maintenance of Research Potential at Kazimierz Wielki University for PhD students and was also financially supported by the Minister of Education and Science under the programme entitled "Regional Initiative of Excellence" for the years 2024–27, Project No. RID/SP/0048/2024/01.

https://doi.org/10.5194/egusphere-2026-3763
Preprint. Discussion started: 21 July 2026

References

Aalto, J., Harrison, S., and Luoto, M.: Statistical modelling predicts almost complete loss of major periglacial processes in Northern Europe by 2100, Nat Commun, 8, 515, https://doi.org/10.1038/s41467-017-00669-3, 2017.

Abdelmajeed, A. Y. A. and Juszczak, R.: Challenges and Limitations of Remote Sensing Applications in Northern Peatlands: Present and Future Prospects, Remote Sensing, 16, https://doi.org/10.3390/rs16030591, 2024.

Ahti, T., Hämet-Ahti, L., and Jalas, J.: Vegetation zones and their sections in northwestern Europe, Annales Botanici Fennici, 5, 169–211, 1968.

Álvarez-Martínez, J. M., Alba, C. E. del, Marcenò, C., Romero, G. H., and Jiménez-Alfaro, B.: Integrating in-situ data and remote sensing for spatiotemporal assessment of alpine vegetation, Alpine Botany [Preprint], https://doi.org/10.21203/rs.3.rs-8491360/v1, 2026.

Anding, D. and Kauth, R.: Estimation of sea surface temperature from space, Remote Sensing of Environment, 1, 217–220, https://doi.org/10.1016/S0034-4257(70)80002-5, 1970.

Autio, J. and Heikkinen, O.: The climate of northern Finland, Fennia-International Journal of Geography, 180, 2002.

Bartsch, A., Strozzi, T., and Nitze, I.: Permafrost Monitoring from Space, SURVEYS IN GEOPHYSICS, 44, 1579–1613, https://doi.org/10.1007/s10712-023-09770-3, 2023.

Bates, D., Mächler, M., Bolker, B., and Walker, S.: Fitting Linear Mixed-Effects Models Using **lme4**, J. Stat. Soft., 67, https://doi.org/10.18637/jss.v067.i01, 2015.

Berner, L. T., Massey, R., Jantz, P., Forbes, B. C., Macias-Fauria, M., Myers-Smith, I., Kumpula, T., Gauthier, G., Andreu-Hayles, L., Gaglioti, B. V., Burns, P., Zetterberg, P., D'Arrigo, R., and Goetz, S. J.: Summer warming explains widespread but not uniform greening in the Arctic tundra biome, Nat Commun, 11, 4621, https://doi.org/10.1038/s41467-020-18479-5, 2020.

Biskaborn, B. K., Smith, S. L., Noetzli, J., Matthes, H., Vieira, G., Streletskiy, D. A., Schoeneich, P., Romanovsky, V. E., Lewkowicz, A. G., Abramov, A., Allard, M., Boike, J., Cable, W. L., Christiansen, H. H., Delaloye, R., Diekmann, B., Drozdov, D., Etzelmüller, B., Grosse, G., Guglielmin, M., Ingeman-Nielsen, T., Isaksen, K., Ishikawa, M., Johansson, M., Johannsson, H., Joo, A., Kaverin, D., Kholodov, A., Konstantinov, P., Kröger, T., Lambiel, C., Lanckman, J.-P., Luo, D., Malkova, G., Meiklejohn, I., Moskalenko, N., Oliva, M., Phillips, M., Ramos, M., Sannel, A. B. K., Sergeev, D., Seybold, C., Skryabin, P., Vasiliev, A., Wu, Q., Yoshikawa, K., Zheleznyak, M., and Lantuit, H.: Permafrost is warming at a global scale, Nat Commun, 10, 264, https://doi.org/10.1038/s41467-018-08240-4, 2019.

Borge, A. F., Westermann, S., Solheim, I., and Etzelmüller, B.: Strong degradation of palsas and peat plateaus in northern Norway during the last 60 years, The Cryosphere, 11, 1–16, https://doi.org/10.5194/tc-11-1-2017, 2017.

Bosiö, J., Johansson, M., Callaghan, T. V., Johansen, B., and Christensen, T. R.: Future vegetation changes in thawing subarctic mires and implications for greenhouse gas exchange—a regional assessment, Climatic Change, 115, 379–398, https://doi.org/10.1007/s10584-012-0445-1, 2012.

Chadburn, S. E., Burke, E. J., Cox, P. M., Friedlingstein, P., Hugelius, G., and Westermann, S.: An observation-based constraint on permafrost loss as a function of global warming, Nature Clim Change, 7, 340–344, https://doi.org/10.1038/nclimate3262, 2017.

Chen, Y., Liu, A., and Cheng, X.: Landsat-Based Monitoring of Landscape Dynamics in Arctic Permafrost Region, JOURNAL OF REMOTE SENSING, 2022, https://doi.org/10.34133/2022/9765087, 2022.

Christiansen, H. H., Etzelmüller, B., Isaksen, K., Juliussen, H., Farbrot, H., Humlum, O., Johansson, M., Ingeman-Nielsen, T., Kristensen, L., Hjort, J., Holmlund, P., Sannel, A. B. K., Sigsgaard, C., Åkerman, H. J., Foged, N., Blikra, L. H., Pernosky, M. A., and Ødegård, R. S.: The thermal state of permafrost in the nordic area during the international polar year 2007–2009, Permafrost and Periglacial Processes, 21, 156–181, https://doi.org/10.1002/ppp.687, 2010.

Crichton, K. A., Anderson, K., Charman, D. J., and Gallego-Sala, A.: Seasonal climate drivers of peak NDVI in a series of Arctic peatlands, Science of The Total Environment, 838, 156419, https://doi.org/10.1016/j.scitotenv.2022.156419, 2022.

Crichton, K. A., Anderson, K., Fewster, R. E., Charman, D. J., Garneau, M., Väliranta, M., Mleczko, M., Handley, J. N., Hodson, S., Parker, R. E., Swindles, G. T., Blaauw, M., and Gallego-Sala, A. V.: Satellite data indicates recent Arctic peatland expansion with warming, Commun Earth Environ, 6, 461, https://doi.org/10.1038/s43247-025-02375-1, 2025.

Czapiewski, S. and Szumińska, D.: An Overview of Remote Sensing Data Applications in Peatland Research Based on Works from the Period 2010–2021, Land, 11, 24, https://doi.org/10.3390/land11010024, 2022.

Demarquet, Q., Rapinel, S., Dufour, S., and Hubert-Moy, L.: Long-Term Wetland Monitoring Using the Landsat Archive: A Review, Remote Sensing, 15, https://doi.org/10.3390/rs15030820, 2023.

Duncan, B. N., Ott, L. E., Abshire, J. B., Brucker, L., Carroll, M. L., Carton, J., Comiso, J. C., Dinnat, E. P., Forbes, B. C., Gonsamo, A., Gregg, W. W., Hall, D. K., Ialongo, I., Jandt, R., Kahn, R. A., Karpechko, A., Kawa, S. R., Kato, S., Kumpula, T., Kyrölä, E., Loboda, T. V., McDonald, K. C., Montesano, P. M., Nassar, R., Neigh, C. S. R., Parkinson, C. L., Poulter, B., Pulliainen, J., Rautiainen, K., Rogers, B. M., Rousseaux, C. S., Soja, A. J., Steiner, N., Tamminen, J., Taylor, P. C., Tzortziou, M. A., Virta, H., Wang, J. S., Watts, J. D., Winker, D. M., and Wu, D. L.: Space-Based Observations for Understanding Changes in the Arctic-Boreal Zone, Reviews of Geophysics, 58, e2019RG000652, https://doi.org/10.1029/2019RG000652, 2020.

Fewster, R. E., Morris, P. J., Ivanovic, R. F., Swindles, G. T., Peregon, A. M., and Smith, C. J.: Imminent loss of climate space for permafrost peatlands in Europe and Western Siberia, Nat. Clim. Chang., 12, 373–379, https://doi.org/10.1038/s41558-022-01296-7, 2022.

Finnish Environment Institute (SYKE): https://ckan.ymparisto.fi/dataset/maanpeite-soilla-ja-rantakosteikoilla, last access: 8 July 2025.

Finnish Meteorological Institute: https://en.ilmatieteenlaitos.fi/statistics-from-1961-onwards, last access: 3 April 2025.

Fronzek, S., Luoto, M., and Carter, T. R.: Potential effect of climate change on the distribution of palsa mires in subarctic Fennoscandia, Climate Research, 32, 1–12, https://doi.org/10.3354/cr032001, 2006.

https://doi.org/10.5194/egusphere-2026-3763
Preprint. Discussion started: 21 July 2026

Gallego-Sala, A. V., Charman, D. J., Brewer, S., Page, S. E., Prentice, I. C., Friedlingstein, P., Moreton, S., Amesbury, M. J., Beilman, D. W., Björck, S., Blyakharchuk, T., Bochicchio, C., Booth, R. K., Bunbury, J., Camill, P., Carless, D., Chimner, R. A., Clifford, M., Cressey, E., Courtney-Mustaphi, C., De Vleeschouwer, F., de Jong, R., Fialkiewicz-Koziel, B., Finkelstein, S. A., Garneau, M., Githumbi, E., Hribjlan, J., Holmquist, J., Hughes, P. D. M., Jones, C., Jones, M. C., Karofeld, E., Klein, E. S., Kokfelt, U., Korhola, A., Lacourse, T., Le Roux, G., Lamentowicz, M., Large, D., Lavoie, M., Loisel, J., Mackay, H., MacDonald, G. M., Makila, M., Magnan, G., Marchant, R., Marcisz, K., Martínez Cortizas, A., Massa, C., Mathijssen, P., Mauquoy, D., Mighall, T., Mitchell, F. J. G., Moss, P., Nichols, J., Oksanen, P. O., Orme, L., Packalen, M. S., Robinson, S., Roland, T. P., Sanderson, N. K., Sannel, A. B. K., Silva-Sánchez, N., Steinberg, N., Swindles, G. T., Turner, T. E., Uglow, J., Väliranta, M., van Bellen, S., van der Linden, M., van Geel, B., Wang, G., Yu, Z., Zaragoza-Castells, J., and Zhao, Y.: Latitudinal limits to the predicted increase of the peatland carbon sink with warming, Nature Clim Change, 8, 907–913, https://doi.org/10.1038/s41558-018-0271-1, 2018.

Gao, B.: NDWI—A normalized difference water index for remote sensing of vegetation liquid water from space, Remote Sensing of Environment, 58, 257–266, https://doi.org/10.1016/S0034-4257(96)00067-3, 1996.

Giese, L., Baumberger, M., Ludwig, M., Schneidereit, H., Sánchez, E., Robroek, B. J. M., Lamentowicz, M., Lehmann, J. R. K., Hölzel, N., Knorr, K.-H., and Meyer, H.: Recent trends in moisture conditions across European peatlands, Remote Sensing Applications: Society and Environment, 37, 101385, https://doi.org/10.1016/j.rsase.2024.101385, 2025.

Gisnås, K., Etzelmüller, B., Lussana, C., Hjort, J., Sannel, A. B. K., Isaksen, K., Westermann, S., Kuhry, P., Christiansen, H. H., Frampton, A., and Åkerman, J.: Permafrost Map for Norway, Sweden and Finland, Permafrost and Periglacial Processes, 28, 359–378, https://doi.org/10.1002/ppp.1922, 2017.

Hammer, Ø., Harper, D. A. T., and Ryan, P. D.: PAST: Paleontological statistics software package for education and data analysis, Palaeontologia Electronica 4(1): 9pp, https://doi.org/http://palaeo-electronica.org/2001_1/past/issue1_01.htm, 2001.

Heijmans, M. M. P. D., Magnússon, R. Í., Lara, M. J., Frost, G. V., Myers-Smith, I. H., van Huissteden, J., Jorgenson, M. T., Fedorov, A. N., Epstein, H. E., Lawrence, D. M., and Limpens, J.: Tundra vegetation change and impacts on permafrost, Nat Rev Earth Environ, 3, 68–84, https://doi.org/10.1038/s43017-021-00233-0, 2022.

Helbig, M., Waddington, J. M., Alekseychik, P., Amiro, B. D., Aurela, M., Barr, A. G., Black, T. A., Blanken, P. D., Carey, S. K., Chen, J., Chi, J., Desai, A. R., Dunn, A., Euskirchen, E. S., Flanagan, L. B., Forbrich, I., Friborg, T., Grelle, A., Harder, S., Heliasz, M., Humphreys, E. R., Ikawa, H., Isabelle, P.-E., Iwata, H., Jassal, R., Korkiakoski, M., Kurbatova, J., Kutzbach, L., Lindroth, A., Löfvenius, M. O., Lohila, A., Mammarella, I., Marsh, P., Maximov, T., Melton, J. R., Moore, P. A., Nadeau, D. F., Nicholls, E. M., Nilsson, M. B., Ohta, T., Peichl, M., Petrone, R. M., Petrov, R., Prokushkin, A., Quinton, W. L., Reed, D. E., Roulet, N. T., Runkle, B. R. K., Sonnentag, O., Strachan, I. B., Taillardat, P., Tuittila, E.-S., Tuovinen, J.-P., Turner, J., Ueyama, M., Varlagin, A., Wilmking, M., Wofsy, S. C., and Zyrianov, V.: Increasing contribution of peatlands to boreal evapotranspiration in a warming climate, Nat. Clim. Chang., 10, 555–560, https://doi.org/10.1038/s41558-020-0763-7, 2020.

Hjort, J. and Luoto, M.: Modelling patterned ground distribution in finnish lapland: an integration of topographical, ground and remote sensing information, Geografiska Annaler: Series A, Physical Geography, 88, 19–29, https://doi.org/10.1111/j.0435-3676.2006.00280.x, 2006.

Hjort, J., Streletskiy, D., Doré, G., Wu, Q., Bjella, K., and Luoto, M.: Impacts of permafrost degradation on infrastructure, Nat Rev Earth Environ, 3, 24–38, https://doi.org/10.1038/s43017-021-00247-8, 2022.

Hugelius, G., Loisel, J., Chadburn, S., Jackson, R. B., Jones, M., MacDonald, G., Marushchak, M., Olefeldt, D., Packalen, M., Siewert, M. B., Treat, C., Turetsky, M., Voigt, C., and Yu, Z.: Large stocks of peatland carbon and nitrogen are vulnerable to permafrost thaw, Proceedings of the National Academy of Sciences, 117, 20438–20446, https://doi.org/10.1073/pnas.1916387117, 2020.

https://doi.org/10.5194/egusphere-2026-3763
Preprint. Discussion started: 21 July 2026

Ikkala, L., Ismail, Wolff, F., Marttila, H., Ronkanen, A.-K., Alekseychik, P., Rana, P., Kohv, M., Tahvanainen, T., Tolvanen, A., Haghighi, A. T., Kumpula, T., Osborne, C., Ilmonen, J., Haapalehto, T., Kløve, B., and Räsänen, A.: Remote sensing applications for monitoring restoration outcomes in boreal forestry-drained peatlands - Reviewed applications and future potential, Remote Sensing of Environment, 333, 115093, https://doi.org/10.1016/j.rse.2025.115093, 2026.

Jimenez, J.-C. and Sobrino, J.: A generalized single-channel method for retrieving land surface temperature from remote sensing data (vol 109, art no D08112, 2004), Journal of Geophysical Research, 108, https://doi.org/10.1029/2003JD003480, 2003.

Jin, H., Huang, Y., Bense, V. F., Ma, Q., Marchenko, S. S., Shepelev, V. V., Hu, Y., Liang, S., Spektor, V. V., Jin, X., Li, X., and Li, X.: Permafrost Degradation and Its Hydrogeological Impacts, Water, 14, 372, https://doi.org/10.3390/w14030372, 2022.

Jin, X.-Y., Jin, H.-J., Iwahana, G., Marchenko, S. S., Luo, D.-L., Li, X.-Y., and Liang, S.-H.: Impacts of climate-induced permafrost degradation on vegetation: A review, Advances in Climate Change Research, 12, 29–47, https://doi.org/10.1016/j.accre.2020.07.002, 2021.

Jones, B. M., Grosse, G., Arp, C. D., Jones, M. C., Walter Anthony, K. M., and Romanovsky, V. E.: Modern thermokarst lake dynamics in the continuous permafrost zone, northern Seward Peninsula, Alaska, Journal of Geophysical Research: Biogeosciences, 116, https://doi.org/10.1029/2011JG001666, 2011.

Joosten, H. and Clarke, D.: Wise use of mires and peatlands: Background and principles including a framework for decision-making, International Mire Conservation Group and International Peat Society, Jyväskylä, Finland, 2002.

Jorgenson, M. T. and Grosse, G.: Remote Sensing of Landscape Change in Permafrost Regions, Permafrost and Periglacial Processes, 27, 324–338, https://doi.org/10.1002/ppp.1914, 2016.

Jóźwik, J. K., Kozioł, K., Frankowski, M., Jakubiak, M., Nowiński, K., Jędrysek, M., Szumińska, D., and Polkowska, Ż.: Does Palsa Thaw in Northern Finland Contribute to Remobilisation of Metals Accumulated in Peat Into Surface Waters?, Land Degradation & Development, n/a, https://doi.org/10.1002/ldr.70370, 2025.

Ju, J. and Roy, D. P.: The availability of cloud-free Landsat ETM+ data over the conterminous United States and globally, Remote Sensing of Environment, 112, 1196–1211, https://doi.org/10.1016/j.rse.2007.08.011, 2008.

Kolari, T. H. M., Sallinen, A., Wolff, F., Kumpula, T., Tolonen, K., and Tahvanainen, T.: Ongoing Fen–Bog Transition in a Boreal Aapa Mire Inferred from Repeated Field Sampling, Aerial Images, and Landsat Data, Ecosystems, 25, 1166–1188, https://doi.org/10.1007/s10021-021-00708-7, 2022.

Krüger, J. P., Conen, F., Leifeld, J., and Alewell, C.: Palsa Uplift Identified by Stable Isotope Depth Profiles and Relation of δ15N to C/N Ratio, Permafrost and Periglacial Processes, 28, 485–492, https://doi.org/10.1002/ppp.1936, 2017.

Kujala, K., Seppälä, M., and Holappa, T.: Physical properties of peat and palsa formation, Cold Regions Science and Technology, 52, 408–414, https://doi.org/10.1016/j.coldregions.2007.08.002, 2008.

Kuznetsova, A., Brockhoff, P. B., and Christensen, R. H. B.: **lmerTest** Package: Tests in Linear Mixed Effects Models, J. Stat. Soft., 82, https://doi.org/10.18637/jss.v082.i13, 2017.

Langer, M., Westermann, S., and Boike, J.: Spatial and temporal variations of summer surface temperatures of wet polygonal tundra in Siberia - implications for MODIS LST based permafrost monitoring, Remote Sensing of Environment, 114, 2059–2069, https://doi.org/10.1016/j.rse.2010.04.012, 2010.

https://doi.org/10.5194/egusphere-2026-3763
Preprint. Discussion started: 21 July 2026

Larson, J., Lidberg, W., Ågren, A. M., and Laudon, H.: Predicting soil moisture conditions across a heterogeneous boreal catchment using terrain indices, Hydrology and Earth System Sciences, 26, 4837–4851, https://doi.org/10.5194/hess-26-4837-2022, 2022.

Laurent, M., Baysinger, M. R., Schaller, J., Lück, M., Hoffmann, M., Windirsch, T., Ellerbrock, R. H., Strauss, J., and Treat, C. C.: Enhanced CO_2 emissions driven by flooding in a simulation of palsa degradation, Biogeosciences, 22, 7881–7899, https://doi.org/10.5194/bg-22-7881-2025, 2025.

Lenth, R. V., Piaskowski, J., Banfai, B., Bolker, B., Buerkner, P., Giné-Vázquez, I., Hervé, M., Jung, M., Love, J., Miguez, F., Riebl, H., and Singmann, H.: Emmeans: Estimated Marginal Means, aka Least-Squares Means, 2026.

Leppiniemi, O., Karjalainen, O., Aalto, J., Luoto, M., and Hjort, J.: Environmental spaces for palsas and peat plateaus are disappearing at a circumpolar scale, The Cryosphere, 17, 3157–3176, https://doi.org/10.5194/tc-17-3157-2023, 2023.

Leppiniemi, O., Karjalainen, O., Aalto, J., Luoto, M., and Hjort, J.: Environmental Drivers of Palsa and Peat Plateau Occurrences: A Regional Comparison Across the Northern Hemisphere, Permafrost and Periglacial Processes, 36, 37–50, https://doi.org/10.1002/ppp.2253, 2025a.

Leppiniemi, O., Karjalainen, O., Aalto, J., Yletyinen, E., Luoto, M., and Hjort, J.: The morpho-ecological state of palsa mires in sub-arctic Fennoscandia: insights from high-resolution spatial modelling, CATENA, 257, 109203, https://doi.org/10.1016/j.catena.2025.109203, 2025b.

Li, W., Zhang, K., Wu, X., Cheng, X., Wang, X., Zhou, Z., Hao, J., and Zhang, X.: Lake changes and their driving factors in circum-arctic permafrost regions from 1990 to 2022, Ecological Indicators, 163, 112066, https://doi.org/10.1016/j.ecolind.2024.112066, 2024.

Liljedahl, A. K., Boike, J., Daanen, R. P., Fedorov, A. N., Frost, G. V., Grosse, G., Hinzman, L. D., Iijma, Y., Jorgenson, J. C., Matveyeva, N., Necsoiu, M., Raynolds, M. K., Romanovsky, V. E., Schulla, J., Tape, K. D., Walker, D. A., Wilson, C. J., Yabuki, H., and Zona, D.: Pan-Arctic ice-wedge degradation in warming permafrost and its influence on tundra hydrology, Nature Geosci, 9, 312–318, https://doi.org/10.1038/ngeo2674, 2016.

Liu, Y., Qiu, H., Wang, N., Yang, D., Zhao, K., Yang, G., Huangfu, W., and Luo, W.: Thermokarst disturbance responses to climate change across the circumpolar permafrost regions from 1990 to 2023, Geoscience Frontiers, 16, 102147, https://doi.org/10.1016/j.gsf.2025.102147, 2025.

Loranty, M. M., Goetz, S. J., and Beck, P. S. A.: Tundra vegetation effects on pan-Arctic albedo, Environ. Res. Lett., 6, 024014, https://doi.org/10.1088/1748-9326/6/2/024014, 2011.

Luoto, M., Heikkinen, R. K., and Carter, T. R.: Loss of palsa mires in Europe and biological consequences, Environmental Conservation, 31, 30–37, https://doi.org/10.1017/S0376892904001018, 2004a.

Luoto, M., Fronzek, S., and Zuidhoff, F. S.: Spatial modelling of palsa mires in relation to climate in northern Europe, Earth Surface Processes and Landforms, 29, 1373–1387, https://doi.org/10.1002/esp.1099, 2004b.

Mamet, S. D., Chun, K. P., Kershaw, G. G. L., Loranty, M. M., and Peter Kershaw, G.: Recent Increases in Permafrost Thaw Rates and Areal Loss of Palsas in the Western Northwest Territories, Canada, Permafrost and Periglacial Processes, 28, 619–633, https://doi.org/10.1002/ppp.1951, 2017.

McFeeters, S. K.: The use of the Normalized Difference Water Index (NDWI) in the delineation of open water features, International Journal of Remote Sensing, 17, 1425–1432, https://doi.org/10.1080/01431169608948714, 1996.

https://doi.org/10.5194/egusphere-2026-3763
Preprint. Discussion started: 21 July 2026

Muir, G., Brown, G. S., Balasubramaniam, K., and Hu, B.: Active layer thermal regime varies across landforms in a subarctic wetland, FACETS, 10, 1–14, https://doi.org/10.1139/facets-2024-0250, 2025.

Murphy, P. N. C., Ogilvie, J., and Arp, P.: Topographic modelling of soil moisture conditions: a comparison and verification of two models, European Journal of Soil Science, 60, 94–109, https://doi.org/10.1111/j.1365-2389.2008.01094.x, 2009.

Myers-Smith, I. H., Kerby, J. T., Phoenix, G. K., Bjerke, J. W., Epstein, H. E., Assmann, J. J., John, C., Andreu-Hayles, L., Angers-Blondin, S., Beck, P. S. A., Berner, L. T., Bhatt, U. S., Bjorkman, A. D., Blok, D., Bryn, A., Christiansen, C. T., Cornelissen, J. H. C., Cunliffe, A. M., Elmendorf, S. C., Forbes, B. C., Goetz, S. J., Hollister, R. D., de Jong, R., Loranty, M. M., Macias-Fauria, M., Maseyk, K., Normand, S., Olofsson, J., Parker, T. C., Parmentier, F.-J. W., Post, E., Schaepman-Strub, G., Stordal, F., Sullivan, P. F., Thomas, H. J. D., Tømmervik, H., Treharne, R., Tweedie, C. E., Walker, D. A., Wilmking, M., and Wipf, S.: Complexity revealed in the greening of the Arctic, Nat. Clim. Chang., 10, 106–117, https://doi.org/10.1038/s41558-019-0688-1, 2020.

National Land Survey of Finland: https://www.maanmittauslaitos.fi/en/maps-and-spatial-data/datasets-and-interfaces/product-descriptions/elevation-model-2-m, last access: 27 August 2025.

Natural Earth: https://www.naturalearthdata.com/, last access: 27 May 2026.

Nedbal, V., Láska, K., and Brom, J.: Mitigation of Arctic Tundra Surface Warming by Plant Evapotranspiration: Complete Energy Balance Component Estimation Using LANDSAT Satellite Data, Remote Sensing, 12, https://doi.org/10.3390/rs12203395, 2020.

Nitze, I. and Grosse, G.: Detection of landscape dynamics in the Arctic Lena Delta with temporally dense Landsat time-series stacks, Remote Sensing of Environment, 181, 27–41, https://doi.org/10.1016/j.rse.2016.03.038, 2016.

Nitze, I., Grosse, G., Jones, B., Romanovsky, V., and Boike, J.: Remote sensing quantifies widespread abundance of permafrost region disturbances across the Arctic and Subarctic, Nature Communications, 9, https://doi.org/10.1038/s41467-018-07663-3, 2018.

Oksanen, J., Simpson, G., Blanchet, F. G., Kindt, R., Legendre, P., Minchin, P., hara, R., Solymos, P., STEVENS, H., Szöcs, E., Wagner, H., Barbour, M., Bedward, M., Bolker, B., Borcard, D., Carvalho, G., Chirico, M., De Cáceres, M., Durand, S., and Weedon, J.: vegan community ecology package version 2.6-2 April 2022, 2022.

Olvmo, M., Holmer, B., Thorsson, S., Reese, H., and Lindberg, F.: Sub-arctic palsa degradation and the role of climatic drivers in the largest coherent palsa mire complex in Sweden (Vissátvuopmi), 1955–2016, Sci Rep, 10, 8937, https://doi.org/10.1038/s41598-020-65719-1, 2020.

Peel, M. C., Finlayson, B. L., and McMahon, T. A.: Updated world map of the Köppen-Geiger climate classification, Hydrology and Earth System Sciences, 11, 1633–1644, https://doi.org/10.5194/hess-11-1633-2007, 2007.

Pettorelli, N., Laurance, W. F., O'Brien, T. G., Wegmann, M., Nagendra, H., and Turner, W.: Satellite remote sensing for applied ecologists: opportunities and challenges, Journal of Applied Ecology, 51, 839–848, https://doi.org/10.1111/1365-2664.12261, 2014.

Philipp, M., Dietz, A., Buchelt, S., and Kuenzer, C.: Trends in Satellite Earth Observation for Permafrost Related Analyses—A Review, Remote Sensing, 13, 1217, https://doi.org/10.3390/rs13061217, 2021.

Piilo, S. R., Korhola, A., Heiskanen, L., Tuovinen, J.-P., Aurela, M., Juutinen, S., Marttila, H., Saari, M., Tuittila, E.-S., Turunen, J., and Väliranta, M. M.: Spatially varying peatland initiation, Holocene development, carbon accumulation patterns and radiative forcing within a subarctic fen, Quaternary Science Reviews, 248, 106596, https://doi.org/10.1016/j.quascirev.2020.106596, 2020.

Pinheiro, J. C. and Bates, D. M.: Mixed-Effects Models in Sand S-PLUS, Springer New York, New York, NY, https://doi.org/10.1007/978-1-4419-0318-1, 2000.

Qiu, C., Ciais, P., Zhu, D., Guenet, B., Chang, J., Chaudhary, N., Kleinen, T., Li, X., Müller, J., Xi, Y., Zhang, W., Ballantyne, A., Brewer, S. C., Brovkin, V., Charman, D. J., Gustafson, A., Gallego-Sala, A. V., Gasser, T., Holden, J., Joos, F., Kwon, M. J., Lauerwald, R., Miller, P. A., Peng, S., Page, S., Smith, B., Stocker, B. D., Sannel, A. B. K., Salmon, E., Schurgers, G., Shurpali, N. J., Wårlind, D., and Westermann, S.: A strong mitigation scenario maintains climate neutrality of northern peatlands, One Earth, 5, 86–97, https://doi.org/10.1016/j.oneear.2021.12.008, 2022.

R Core Team.: https://www.scirp.org/reference/referencespapers?referenceid=3967248, last access: 24 April 2025.

Rahimi, E. and Jung, C.: Evaluating the applicability of landsat 8 data for global time series analysis, Front. Remote Sens., 5, https://doi.org/10.3389/frsen.2024.1492534, 2024.

Rantanen, M., Karpechko, A. Y., Lipponen, A., Nordling, K., Hyvärinen, O., Ruosteenoja, K., Vihma, T., and Laaksonen, A.: The Arctic has warmed nearly four times faster than the globe since 1979, Commun Earth Environ, 3, 1–10, https://doi.org/10.1038/s43247-022-00498-3, 2022.

Rouse, J. W., Haas, R. H., Schell, J. A., and Deering, D. W.: Monitoring vegetation systems in the Great Plains with ERTS, NASA. Goddard Space Flight Center 3d ERTS-1 Symp., Vol. 1, Sect. A, 1974.

Roy, D. P., Wulder, M. A., Loveland, T. R., C.e., W., Allen, R. G., Anderson, M. C., Helder, D., Irons, J. R., Johnson, D. M., Kennedy, R., Scambos, T. A., Schaaf, C. B., Schott, J. R., Sheng, Y., Vermote, E. F., Belward, A. S., Bindschadler, R., Cohen, W. B., Gao, F., Hipple, J. D., Hostert, P., Huntington, J., Justice, C. O., Kilic, A., Kovalskyy, V., Lee, Z. P., Lymburner, L., Masek, J. G., McCorkel, J., Shuai, Y., Trezza, R., Vogelmann, J., Wynne, R. H., and Zhu, Z.: Landsat-8: Science and product vision for terrestrial global change research, Remote Sensing of Environment, 145, 154–172, https://doi.org/10.1016/j.rse.2014.02.001, 2014.

Roy, D. P., Kovalskyy, V., Zhang, H. K., Vermote, E. F., Yan, L., Kumar, S. S., and Egorov, A.: Characterization of Landsat-7 to Landsat-8 reflective wavelength and normalized difference vegetation index continuity, Remote Sensing of Environment, 185, 57–70, https://doi.org/10.1016/j.rse.2015.12.024, 2016.

Schuur, E., McGuire, A. D., Schädel, C., Grosse, G., Harden, J., Hayes, D. J., Hugelius, G., Koven, C., Kuhry, P., Lawrence, D., Natali, S., Olefeldt, D., Romanovsky, V., Schaefer, K., Turetsky, M., Treat, C., and Vonk, J.: Climate change and the permafrost carbon feedback, Nature, 2015, 171–179, https://doi.org/10.1038/nature14338, 2015.

Schuur, E. A. G., Bockheim, J., Canadell, J. G., Euskirchen, E., Field, C. B., Goryachkin, S. V., Hagemann, S., Kuhry, P., Lafleur, P. M., Lee, H., Mazhitova, G., Nelson, F. E., Rinke, A., Romanovsky, V. E., Shiklomanov, N., Tarnocai, C., Venevsky, S., Vogel, J. G., and Zimov, S. A.: Vulnerability of Permafrost Carbon to Climate Change: Implications for the Global Carbon Cycle, BioScience, 58, 701–714, https://doi.org/10.1641/B580807, 2008.

Schuur, E. A. G., Abbott, B. W., Commane, R., Ernakovich, J., Euskirchen, E., Hugelius, G., Grosse, G., Jones, M., Koven, C., Leshyk, V., Lawrence, D., Loranty, M. M., Mauritz, M., Olefeldt, D., Natali, S., Rodenhizer, H., Salmon, V., Schädel, C., Strauss, J., Treat, C., and Turetsky, M.: Permafrost and Climate Change: Carbon Cycle Feedbacks From the Warming Arctic, Annual Review of Environment and Resources, 47, 343–371, https://doi.org/10.1146/annurev-environ-012220-011847, 2022.

Seo, M. and Kim, H.-C.: Arctic Greening Trends: Change Points in Satellite-Derived Normalized Difference Vegetation Indexes and Their Correlation with Climate Variables over the Last Two Decades, Remote Sensing, 16, 1160, https://doi.org/10.3390/rs16071160, 2024.

Seppälä, M.: The Origin of Palsas, Geografiska Annaler: Series A, Physical Geography, 68, 141–147, https://doi.org/10.1080/04353676.1986.11880167, 1986.

Seppälä, M.: Palsa mires in Finland, in: Finland - land of mires, Finnish Environment Institute, Helsinki, 155–162, 2006.

Seppälä, M.: Synthesis of studies of palsa formation underlining the importance of local environmental and physical characteristics, Quaternary Research, 75, 366–370, https://doi.org/10.1016/j.yqres.2010.09.007, 2011.

Shang, Y., Cheng, B., Zhang, Z., Wang, Q., Jin, P., Huang, L., Liu, C., Huang, L., Ding, X., Shen, T., Tang, B.-H., and Gu, Y.: Artificial Intelligence for Remote Sensing: Progress, Challenges, and Perspectives, IEEE Journal of Selected Topics in Applied Earth Observations and Remote Sensing, 19, 6840–6874, https://doi.org/10.1109/JSTARS.2026.3656185, 2026.

Shijin, W. and Xiaoqing, P.: Permafrost degradation services for Arctic greening, CATENA, 229, 107209, https://doi.org/10.1016/j.catena.2023.107209, 2023.

Sim, T. G., Swindles, G. T., Morris, P. J., Baird, A. J., Cooper, C. L., Gallego-Sala, A. V., Charman, D. J., Roland, T. P., Borken, W., Mullan, D. J., Aquino-López, M. A., and Gałka, M.: Divergent responses of permafrost peatlands to recent climate change, Environ. Res. Lett., 16, 034001, https://doi.org/10.1088/1748-9326/abe00b, 2021.

Sjögersten, S., Ledger, M., Siewert, M., de la Barreda-Bautista, B., Sowter, A., Gee, D., Foody, G., and Boyd, D. S.: Optical and radar Earth observation data for upscaling methane emissions linked to permafrost degradation in sub-Arctic peatlands in northern Sweden, Biogeosciences, 20, 4221–4239, https://doi.org/10.5194/bg-20-4221-2023, 2023.

Smith, S. L., O'Neill, H. B., Isaksen, K., Noetzli, J., and Romanovsky, V. E.: The changing thermal state of permafrost, Nat Rev Earth Environ, 3, 10–23, https://doi.org/10.1038/s43017-021-00240-1, 2022.

Sollid, J. L. and Sørbel, L.: Palsa Bogs as a Climate Indicator: Examples from Dovrefjell, Southern Norway, Ambio, 27, 287–291, 1998.

Song, C., Woodcock, C. E., Seto, K. C., Lenney, M. P., and Macomber, S. A.: Classification and Change Detection Using Landsat TM Data: When and How to Correct Atmospheric Effects?, Remote Sensing of Environment, 75, 230–244, https://doi.org/10.1016/S0034-4257(00)00169-3, 2001.

Streletskiy, D., Anisimov, O., and Vasiliev, A.: Permafrost Degradation, in: Snow and Ice-Related Hazards, Risks, and Disasters, edited by: Shroder, J. F., Haeberli, W., and Whiteman, C., Academic Press, Boston, 303–344, https://doi.org/10.1016/B978-0-12-394849-6.00010-X, 2015.

Tikkanen, M.: The changing landforms of Finland, Fennia - International Journal of Geography, 180, 21–30, 2002.

Turetsky, M. R., Abbott, B. W., Jones, M. C., Anthony, K. W., Olefeldt, D., Schuur, E. A. G., Grosse, G., Kuhry, P., Hugelius, G., Koven, C., Lawrence, D. M., Gibson, C., Sannel, A. B. K., and McGuire, A. D.: Carbon release through abrupt permafrost thaw, Nat. Geosci., 13, 138–143, https://doi.org/10.1038/s41561-019-0526-0, 2020.

USGS: https://earthexplorer.usgs.gov/, last access: 12 September 2025.

https://doi.org/10.5194/egusphere-2026-3763
Preprint. Discussion started: 21 July 2026

Verdonen, M., Störmer, A., Lotsari, E., Korpelainen, P., Burkhard, B., Colpaert, A., and Kumpula, T.: Permafrost degradation at two monitored palsa mires in north-west Finland, The Cryosphere, 17, 1803–1819, https://doi.org/10.5194/tc-17-1803-2023, 2023.

Verdonen, M., Villoslada, M., Kolari, T. H. M., Tahvanainen, T., Korpelainen, P., Tarolli, P., and Kumpula, T.: Spatial Distribution of Thaw Depth in Palsas Estimated From Optical Unoccupied Aerial Systems Data, Permafrost and Periglacial Processes, n/a, https://doi.org/10.1002/ppp.2252, 2024.

Wenzl, M., Baumhoer, C. A., Dietz, A. J., and Kuenzer, C.: Vegetation Changes in the Arctic: A Review of Earth Observation Applications, Remote Sensing, 16, 4509, https://doi.org/10.3390/rs16234509, 2024.

Westermann, S., Langer, M., and Boike, J.: Spatial and temporal variations of summer surface temperatures of high-arctic tundra on Svalbard — Implications for MODIS LST based permafrost monitoring, Remote Sensing of Environment, 115, 908–922, https://doi.org/10.1016/j.rse.2010.11.018, 2011.

Worrall, F., Boothroyd, I. M., Gardner, R. L., Howden, N. J. K., Burt, T. P., Smith, R., Mitchell, L., Kohler, T., and Gregg, R.: The Impact of Peatland Restoration on Local Climate: Restoration of a Cool Humid Island, Journal of Geophysical Research: Biogeosciences, 124, 1696–1713, https://doi.org/10.1029/2019JG005156, 2019.

Wulder, M. A., Masek, J. G., Cohen, W. B., Loveland, T. R., and Woodcock, C. E.: Opening the archive: How free data has enabled the science and monitoring promise of Landsat, Remote Sensing of Environment, 122, 2–10, https://doi.org/10.1016/j.rse.2012.01.010, 2012.

Wulder, M. A., Loveland, T. R., Roy, D. P., Crawford, C. J., Masek, J. G., Woodcock, C. E., Allen, R. G., Anderson, M. C., Belward, A. S., Cohen, W. B., Dwyer, J., Erb, A., Gao, F., Griffiths, P., Helder, D., Hermosilla, T., Hipple, J. D., Hostert, P., Hughes, M. J., Huntington, J., Johnson, D. M., Kennedy, R., Kilic, A., Li, Z., Lymburner, L., McCorkel, J., Pahlevan, N., Scambos, T. A., Schaaf, C., Schott, J. R., Sheng, Y., Storey, J., Vermote, E., Vogelmann, J., White, J. C., Wynne, R. H., and Zhu, Z.: Current status of Landsat program, science, and applications, Remote Sensing of Environment, 225, 127–147, https://doi.org/10.1016/j.rse.2019.02.015, 2019.

Xu, H.: Modification of normalised difference water index (NDWI) to enhance open water features in remotely sensed imagery, International Journal of Remote Sensing, 27, 3025–3033, https://doi.org/10.1080/01431160600589179, 2006.

Yang, Y., Wang, X., and Wang, T.: Permafrost Degradation Induces the Abrupt Changes of Vegetation NDVI in the Northern Hemisphere, EARTHS FUTURE, 12, https://doi.org/10.1029/2023EF004309, 2024.

Zhao, Y., Samat, A., Du, P., Luo, K., Zhu, E., and Li, W.: Remote Sensing of Non-Intertidal Wetlands: An Overview of Current Status and Future Research Directions, J geovis spat anal, 10, 7, https://doi.org/10.1007/s41651-026-00248-5, 2026.

Zhou, Y., Dong, J., Xiao, X., Xiao, T., Yang, Z., Zhao, G., Zou, Z., and Qin, Y.: Open Surface Water Mapping Algorithms: A Comparison of Water-Related Spectral Indices and Sensors, Water, 9, https://doi.org/10.3390/w9040256, 2017.

Zhu, X. X., Tuia, D., Mou, L., Xia, G.-S., Zhang, L., Xu, F., and Fraundorfer, F.: Deep Learning in Remote Sensing: A Comprehensive Review and List of Resources, IEEE Geoscience and Remote Sensing Magazine, 5, 8–36, https://doi.org/10.1109/MGRS.2017.2762307, 2017.

Zhu, Z., Wulder, M. A., Roy, D. P., Woodcock, C. E., Hansen, M. C., Radeloff, V. C., Healey, S. P., Schaaf, C., Hostert, P., Strobl, P., Pekel, J.-F., Lymburner, L., Pahlevan, N., and Scambos, T. A.: Benefits of the free and open Landsat data policy, Remote Sensing of Environment, 224, 382–385, https://doi.org/10.1016/j.rse.2019.02.016, 2019.